Vibronic coupling of shortlived electronic states

H. Estrada, L. S. Cederbaum, and W. Domcke

Citation: The Journal of Chemical Physics **84**, 152 (1986); doi: 10.1063/1.450165
View online: http://dx.doi.org/10.1063/1.450165
View Table of Contents: http://scitation.aip.org/content/aip/journal/jcp/84/1?ver=pdfcov
Published by the AIP Publishing

Articles you may be interested in

Vibronic coupling mechanism in the Ã2 A 2–B̃2 B 2 excited states of benzyl radical
J. Chem. Phys. **104**, 8896 (1996); 10.1063/1.471659

Effects of vibronic coupling on the local Frenkel states in doped naphthalene crystals
J. Chem. Phys. **104**, 2806 (1996); 10.1063/1.471104

Experimental study of vibrational excitation of allene by slow electron impact: Vibronic coupling in the short lived negative ion states
J. Chem. Phys. **100**, 5588 (1994); 10.1063/1.467126

Photoelectron spectroscopy and electronic structure of clusters of the group V elements. II. Tetramers: Strong Jahn–Teller coupling in the tetrahedral 2 E ground states of P+ 4, As+ 4, and Sb+ 4
J. Chem. Phys. **93**, 6318 (1990); 10.1063/1.459698

Vibronic and electronic states of doubly charged H2S studied by Auger and charge transfer spectroscopy and by a b i n i t i o calculations
J. Chem. Phys. **93**, 918 (1990); 10.1063/1.459118

This article is copyrighted as indicated in the article. Reuse of AIP content is subject to the terms at: http://scitation.aip.org/termsconditions. Downloaded to IP: 130.89.98.137 On: Sun, 30 Nov 2014 02:07:35

Vibronic coupling of short-lived electronic states

H. Estrada,[a] L. S. Cederbaum, and W. Domcke
Theoretische Chemie, Physikalisch-Chemisches Institut, Universität Heidelberg, Im Neuenheimer Feld 253, D-6900 Heidelberg, West Germany

(Received 6 June 1985; accepted 15 July 1985)

The interaction of short-lived electronic states through the nuclear motion is investigated. Particular attention is paid to the impact of this interaction on differential and integrated cross sections for resonant electron–molecule scattering. A vibronic coupling model which has been successfully applied to study vibronic interactions in bound electronic states is extended to resonance states. Calculations of the nuclear dynamics in the nonlocal potential of the coupled resonance states are presented and discussed for several examples including up to two vibrational modes.

I. INTRODUCTION

Resonance states play a central role in many collision phenomena in various fields of physics and chemistry. Resonance effects have been extensively investigated, for example, in reactive and nonreactive atomic and molecular collisions,[1] in molecular photoionization,[2] and in electron–molecule scattering.[3] In the latter case it is commonly assumed that the collision takes place via a single resonance state which does not interact with other possibly existing resonance states. It is well known, however, that electronically bound[4] molecular states often interact with each other through the nuclear motion and it seems natural to investigate this *vibronic coupling*, as it is usually called, also in the case of short-lived electronic states.

In the present work we theoretically investigate the vibronic coupling of resonance states. To be specific we confine ourselves to electron–molecule scattering via shape resonances[3] and investigate elastic scattering and vibrational excitation of the target molecule. It should be noted, however, that this is only a minor restriction. Our main concern is the study of the nuclear dynamics in vibronically coupled resonance states which is formally the same for most kinds of resonance states.

Electron transmission spectra have been reported in the literature for many molecules.[5,6] For polyatomic molecules one often recognizes in these spectra the presence of two or more relatively close-lying resonances. A particularly nice example is the transmission spectrum in *p*-benzoquinone[5,7] which exhibits four discernible resonances within an energy range of less than 4 eV. Energetically close-lying resonance states suggest that vibronic coupling effects between these states might be important and have to be considered. Moreover, since electron transmission spectroscopy is probably insensitive to the detection of broad resonances, we may assume even more resonances to be present which might overlap with the observed ones, thus enhancing the probability for non-Born–Oppenheimer effects to occur.

The intense excitation of single quanta of nontotally symmetric vibrational modes of the target molecule by resonant electron impact gives evidence of the vibronic coupling mechanism in resonances. This kind of excitation has been observed in scattering experiments for many molecules. Examples are benzene[8] and boron trifluoride.[9] Further indication for vibronic coupling in resonances is given by strong geometry changes in resonance states which lower the symmetry of the anion compared to that of the target molecule. There are not many computations on bound and temporary anionic states available in the literature to draw conclusions on whether such changes are rare or common. Prominent examples for strong geometry changes are acetylene and hydrogen cyanide.[10]

A few studies of the interaction between resonances are available in the literature. Mies[11] has been the first to investigate this interaction via coupling to the nonresonant scattering continuum. His model calculations show that remarkable effects are possible for overlapping resonances. The same mechanism has been proposed by Hazi[12] to interpret experiments on dissociative electron attachment to hydrogen bromide. Devdariani *et al.*[13] have more generally investigated the interaction between resonances in the context of atomic collisions using two local models. For completeness we also mention the work by Read[14] and Orgurtsov *et al.*[15] who have investigated vibronic coupling in the target molecule, but not between the resonances.

The general theory of vibronic coupling of resonance states is discussed in the next section. Emphasis is laid on the potential describing the nuclear motion in the vibronically coupled resonance states. In particular, this potential is a nonlocal operator implying that, in general, the nuclear dynamics is extremely tedious to compute for realistic systems and the results obtained are not amenable to interpretation in simple terms. To overcome these difficulties, local approximations are introduced and discussed in Sec. III. In Sec. IV a model which has been successfully applied in vibronic coupling cases of bound states is extended to the case of resonances. Static and dynamic aspects of the model are discussed and, in particular, two-mode nonlocal computations are presented for the first time.

II. GENERAL THEORY OF VIBRONIC COUPLING OF RESONANCE STATES

It is well known that resonance states, or briefly resonances, can be described as discrete states embedded into and

[a] Permanent address: Departamento de Fisica, Universidad Nacional, Bogotá, Columbia, AA 91060.

 0021-9606/86/010152-18$02.10 © 1985 American Institute of Physics

This article is copyrighted as indicated in the article. Reuse of AIP content is subject to the terms at: http://scitation.aip.org/termsconditions. Downloaded to IP: 130.89.98.137 On: Sun, 30 Nov 2014 02:07:35

interacting with a continuum.[16–19] For simplicity we consider only two discrete states $|d_1\rangle$ and $|d_2\rangle$ and a single electronic continuum $|k\rangle$. The generalization to more states is straightforward. All states are chosen to be *diabatic* states,[20,21] i.e., the nuclear kinetic energy does not couple these states. The continuum states are taken to be energy normalized and orthogonal to the discrete states

$$\langle \mathbf{k}|\mathbf{k}'\rangle = \delta(\tfrac{1}{2}k^2 - \tfrac{1}{2}k'^2)\delta(\Omega_k - \Omega_{k'}), \tag{1a}$$

$$\langle d_i|\mathbf{k}\rangle = 0; \quad i = 1,2, \tag{1b}$$

$$\langle d_i|d_j\rangle = \delta_{ij}; \quad i,j = 1,2. \tag{1c}$$

To investigate the vibronic coupling of resonance states we consider the resonant vibrational excitation of molecules by electron scattering. The projection operator formalism of Feshbach[22] provides a convenient tool to compute the corresponding cross section. We introduce, as usual, an operator $\hat{Q}$ which projects on the subset of discrete states

$$\hat{Q} = |d_1\rangle\langle d_1| + |d_2\rangle\langle d_2| \tag{2a}$$

and its complement

$$\hat{P} = 1 - \hat{Q}. \tag{2b}$$

The full Hamiltonian describing the electron-target system is decomposed according to

$$H = H_{PP} + H_{QQ} + H_{QP} + H_{PQ}, \tag{3}$$

where $H_{QP} = QHP$, etc. With the common decomposition (3), the electron–molecule scattering T matrix can be evaluated in analogy to the well-known single resonance case.[23–30] The resonant part of the T matrix reads

$$T(i \to f) = \langle f|H_{PQ}(E - H_{\text{eff}})^{-1}H_{QP}|i\rangle, \tag{4a}$$

$$H_{\text{eff}} = H_{QQ} + H_{QP}(E - H_{PP})^{-1}H_{PQ}, \tag{4b}$$

$|i\rangle$ represents the asymptotic state of the incoming electron and the molecule in its initial state. Analogously, $|f\rangle$ represents the asymptotic state of the outgoing electron and the residual vibrationally excited molecule. E is the total energy which is conserved in the scattering process.

Of course, the full T matrix for the process additively contains a nonresonant term. For inelastic processes this term vanishes if the continuum–continuum interaction W is neglected or if W is independent of the internuclear coordinates. The nonresonant T matrix can be neglected in many cases. In any case the nuclear dynamics in the coupled resonances is described by the resonant T matrix in Eq. (4).

Including the nuclear degrees of freedom we explicitly write for the Hamiltonian

$$H = H_0 + U + V, \tag{5a}$$

$$H_0 = \tilde{H}_0 + |d_1\rangle\epsilon_1\langle d_1| + |d_2\rangle\epsilon_2\langle d_2| + \int k\,dk\,d\Omega_k\,|\mathbf{k}\rangle\epsilon_k\langle \mathbf{k}|, \tag{5b}$$

$$U = |d_1\rangle U_{12}\langle d_2| + \text{h.c.}, \tag{5c}$$

$$V = \int k\,dk\,d\Omega_k\{|d_1\rangle V_{1\mathbf{k}}\langle \mathbf{k}| + |d_2\rangle V_{2\mathbf{k}}\langle \mathbf{k}|\} + \text{h.c.}\ . \tag{5d}$$

The relation between the terms appearing in this Hamiltonian and the four terms on the right-hand side of Eq. (3) is obvious. The first term H_0 of the Hamiltonian describes the nuclear and electronic motion in the uncoupled discrete and continuum states. We suppress for simplicity the translational and rotational degrees of freedom and write

$$\tilde{H}_0 = T_N + V_0(\mathbf{Q}), \tag{5e}$$

where T_N is the nuclear kinetic energy operator and $V_0(\mathbf{Q})$ is the electronic ground state potential energy surface depending on the internuclear coordinates which are collectively denoted by $\mathbf{Q}$. The term U couples the discrete states and the interaction V mixes these states with the continuum and converts them into resonances. Since both discrete states interact with the same continuum, the term V indirectly also couples the discrete states with each other. Thus both U and V give rise to vibronic coupling effects, but the underlying mechanisms are very different.

In principle the Hamiltonian (5) should also contain an interaction W which acts only in the continuum. On the other hand, the influence of this interaction on the resonances can be included by a redefinition of the basis states $|\mathbf{k}\rangle$, i.e., by prediagonalizing the Hamiltonian in the continuum (see, for instance, Ref. 31). In electron–molecule scattering the interaction W gives rise to nonresonant background scattering. There is much experimental evidence[32] that vibrational excitation via resonances is much more effective than via nonresonant processes, except possibly near threshold and in forward scattering. We may thus neglect the dependence of W and of the continuum states $|\mathbf{k}\rangle$ on the internuclear distances $\mathbf{Q}$. The energies ϵ_1 and ϵ_2 of the discrete states and the discrete state–continuum and discrete state–discrete state matrix elements $V_{1\mathbf{k}}$, $V_{2\mathbf{k}}$, and U_{12} depend on the coordinates $\mathbf{Q}$.

To proceed we assume the Born–Oppenheimer or, more precisely, the adiabatic approximation to hold for the target molecular states and write

$$|i\rangle = |\mathbf{k}_i\rangle|\mathbf{0}\rangle|\Phi_0\rangle, \tag{6a}$$

$$|f\rangle = |\mathbf{k}_f\rangle|\mathbf{n}\rangle|\Phi_0\rangle. \tag{6b}$$

$|\mathbf{0}\rangle$ and $|\mathbf{n}\rangle$ denote the target vibrational initial and final states, respectively and $|\Phi_0\rangle$ is the electronic state of the target. The Born–Oppenheimer approximation is usually excellent for molecules in the electronic ground state. In a different context, the impact of deviations from this approximation on the scattering cross sections has been discussed by Read[14,33] and Ogurtsov and Kazantseva.[15,34]

Using the Hamiltonian (5), expression (4), and the ansatz (6), we may eliminate the electronic degrees of freedom from the T matrix which now takes on the form

$$T(i \to f) = \langle \mathbf{n}|\mathbf{V}_{\mathbf{k}_f}^{\dagger}(E\,\mathbf{1} - \mathscr{H})^{-1}\mathbf{V}_{\mathbf{k}_i}|\mathbf{0}\rangle. \tag{7}$$

$\mathbf{V}_{\mathbf{k}}$ is a column vector with elements $V_{1\mathbf{k}}$ and $V_{2\mathbf{k}}$ and the 2×2 unit matrix is devoted by $\mathbf{1}$. $\mathscr{H}$ is an effective Hamiltonian which controls the nuclear dynamics in the coupled resonance states and reads

$$\mathscr{H} = T_N\mathbf{1} + \begin{pmatrix} V_1 + F_{11}(E - \tilde{H}_0) & U_{12} + F_{12}(E - \tilde{H}_0) \\ U_{21} + F_{21}(E - \tilde{H}_0) & V_2 + F_{22}(E - \tilde{H}_0) \end{pmatrix}. \tag{8}$$

$V_1(\mathbf{Q})$ and $V_2(\mathbf{Q})$ denote the *diabatic* potential energy surfaces of the discrete states $|d_1\rangle$ and $|d_2\rangle$, respectively. $U_{12}(Q)$ is the interaction matrix element of these states. The matrix $\mathbf{F} = \{F_{pq}\}$ appears as the result of the interaction of the dis-

This article is copyrighted as indicated in the article. Reuse of AIP content is subject to the terms at: http://scitation.aip.org/termsconditions. Downloaded to IP: 130.89.98.137 On: Sun, 30 Nov 2014 02:07:35

crete states with the continuum and may be called the *level-shift* operator. Its elements are given by $(p,q = 1,2)$

$$F_{pq}(E-\tilde{H}_0) = \Delta_{pq}(E-\tilde{H}_0) - (i/2)\Gamma_{pq}(E-\tilde{H}_0), \quad (9a)$$

$$\Gamma_{pq}(E) = 2\pi \int k\, dk\, d\Omega_k V_{pk}\delta(E-k^2/2)V^*_{qk}, \quad (9b)$$

$$\Delta_{pq}(E) = \frac{P}{2\pi}\int dE' \frac{\Gamma_{pq}(E')}{E-E'}. \quad (9c)$$

P is Cauchy's principal part. The level-shift operator depends explicitly on the nuclear coordinates via the matrix elements $V_{1k}(\mathbf{Q})$ and $V_{2k}(\mathbf{Q})$.

Equations (7)–(9) are the basic equations of this section and deserve some discussion. In the theory of resonant electron–molecule scattering via a single resonance state the nuclear dynamics in this state is governed by an effective Hamiltonian which is identical with a diagonal element of $\mathscr{H}$ in Eq. (8), say $\mathscr{H}_{11}$ (see Refs. 23–30, and 35). The effective potential $V_1(\mathbf{Q}) + F_{11}(E-\tilde{H}_0)$ is complex, energy dependent, and nonlocal. In the case of two and more resonance states, the same effective potentials describe the nuclear dynamics in the *diabatic resonance states*.[63] These states are coupled to each other by two different types of interactions. An interaction U_{12} which depends only on the internuclear coordinates and an interaction F_{12} which is complex, energy dependent, and nonlocal. Without the level-shift operator, $\mathscr{H}$ describes the nuclear motion in vibronically coupled bound states and U_{12} is the corresponding vibronic coupling term (see, e.g., Ref. 37). F_{12} describes the coupling through the common continuum.

In a simple picture, the potential U in Eq. (5) can be viewed as a "hopping" term between the discrete states and the potential V as a hopping term between the continuum and a discrete state. Owing to U, the electron may hop from one discrete state to the other, thus coupling directly these states. V couples the states only indirectly: the electron may hop from one discrete state to the continuum and subsequently into the other discrete state. We speak of *direct* and *indirect vibronic coupling*, respectively. Mies[11] has first studied the interaction of resonances of the same symmetry via the latter coupling mechanism. The same mechanism has been proposed by Hazi[12] to explain the experimental findings in the dissociative electron attachment of HBr. Both coupling mechanisms have also been investigated by Devdariani *et al.*[13] within the Demkov and Nikitin models, which are local models, in the context of atomic collisions.

Experiments indicate that single quanta of nontotally symmetric vibrational modes are often excited in electron–molecule scattering processes.[8,9,32] This fact cannot easily be explained when considering isolated resonances.[8] The vibronic coupling mechanism, however, provides a natural explanation for this observation. In this work we consider a polyatomic molecule which belongs to an abelian point group. We assume two discrete states which transform according to different symmetry representation Γ_1 and Γ_2. These states are coupled through an, obviously nontotally symmetric, mode described by the coordinate Q_u which transforms according to Γ_u. We call this mode the *coupling mode*. Since the Hamiltonian is totally symmetric, the product of the representations of the discrete states and of this mode must contain the totally symmetric representation Γ_g, i.e., the coupling mode obeys the selection rule

$$\Gamma_1 \otimes \Gamma_u \otimes \Gamma_2 \supset \Gamma_g. \quad (10)$$

The interaction matrix element U_{12} also transforms as Γ_u and is an odd function of the coordinate Q_u. Since any molecule possesses at least one totally symmetric mode, we consider in addition such a mode and denote its coordinate Q_g. The vibrational states of the target molecule are now $|n_g n_u\rangle$, where n_g and n_u are quantum numbers of the totally and nontotally symmetric modes, respectively. The extension to nonabelian point groups and the inclusion of additional vibrational modes is straightforward.

The effective Hamiltonian is a 2×2 matrix and, hence, the T matrix (7) can be expressed as a sum of four terms

$$T(i\to f) = T_{11} + T_{22} + T_{12} + T_{21}, \quad (11a)$$

where $(p,q = 1,2)$

$$T_{pq} = \langle n_g n_u | V^*_{pk_f}(E\mathbf{1} - \mathscr{H})^{-1}_{pq} V_{qk_i} | 0,0\rangle. \quad (11b)$$

In contrast to U_{12}, the functional form of the interaction matrix elements V_{pk} is not restricted by symmetry considerations. Since the discrete and continuum states are diabatic states, we assume that the latter elements are slowly varying functions of the internuclear coordinates. For simplicity we take them to be independent of the nontotally symmetric coordinate Q_u, but *not* of Q_g. Actually it suffices to require that the elements V_{pk} are even functions of Q_u in order to derive Eqs. (12)–(17). It should be noted that the widths $\Gamma_{pp}(E) = 2\pi \int d\Omega_k |V_{pk}|^2$ are even functions of Q_u. To investigate the influence of the dependence of V_{pk} on Q_u, one may expand this quantity in powers of Q_u about some reference geometry, which is usually the equilibrium geometry of the target, and repeat the following calculations.

We note that the coupling element $F_{12}(E-\tilde{H}_0)$ appearing in the effective Hamiltonian (8) vanishes because the discrete states have different symmetries [consult Eq. (9)]. Thus, the indirect vibronic coupling mechanism is not effective. Furthermore, since U_{12} is an odd function of Q_u, the diagonal and nondiagonal elements of $\mathscr{H}$ and hence also the corresponding elements of its resolvent transform according to different symmetry representations. Consequently, either T_{11} and T_{22} or T_{12} and T_{21} are equal to zero depending on whether an odd or even number of quanta of the nontotally symmetric mode are excited. The differential cross section for vibrational excitation now reads

$$\left(\frac{d\sigma}{d\Omega}\right)_{n_u\text{even}} = \frac{(2\pi)^4}{k_i^2}|T_{11}+T_{22}|^2, \quad (12a)$$

$$\left(\frac{d\sigma}{d\Omega}\right)_{n_u\text{odd}} = \frac{(2\pi)^4}{k_i^2}|T_{12}+T_{21}|^2. \quad (12b)$$

The number of n_g of totally symmetric quanta is arbitrary. If the target molecule is not in its vibrationless ground state $|0,0\rangle$, but in some excited state $|m_g m_u\rangle$, we may just substitute in Eq. (11b) the former state by the latter one. Then Eqs. (12) hold for $(n_u - m_u)$ being even and odd numbers, respectively.

Once the vibronic coupling mechanism is neglected, i.e., $U_{12} = 0$, the cross section for the excitation of an odd number of nontotally symmetric quanta vanishes. Only even

This article is copyrighted as indicated in the article. Reuse of AIP content is subject to the terms at: http://scitation.aip.org/termsconditions. Downloaded to IP: 130.89.98.137 On: Sun, 30 Nov 2014 02:07:35

quanta of the coupling mode can be excited. The situation changes if the expansion of V_{pk} in Q_u contains odd powers. In this case an odd number of nontotally symmetric quanta can be excited by the resonant process, without vibronic coupling, but we expect the corresponding cross sections to be small. The vibronic coupling mechanism, on the other hand, may lead to substantial cross sections. This is demonstrated by the dynamical calculations of Sec. IV. The situation is somewhat related to that encountered in optical spectroscopy. Within the well-known Condon approximation, where the oscillator strength is taken to be constant in Q, only even quanta of nontotally symmetric modes can be excited.[37] The vibronic coupling mechanism is often found to be responsible for the strong excitation of an odd number of quanta of these modes.[36]

To calculate the integral cross section for each vibrational excitation, we integrate over all final angles of the outgoing electron and average over the orientation of the molecular target. Here and in the following we choose the ground state energy to be the zero point of our energy scale, i.e., $E = k^2/2$ is the kinetic energy of the incoming electron and $\tilde{H}_0$ contains no zero-point energy. The angular dependence of the T matrix is carried by the elements V_{pk}. Because of the different symmetries of the discrete states, integration over the angles of the outgoing electron eliminates the mixed forms $T_{12}T^*_{21}$, $T_{21}T^*_{12}$, $T_{11}T^*_{22}$, and $T_{22}T^*_{11}$. We introduce the new quantities

$$|V_{pE}|^2 = 2\pi \int d\Omega_k |V_{pk}|^2; \quad p = 1,2 \tag{13}$$

and "T-matrix elements" ($p,q = 1,2$)

$$T_{pq}(E) = \langle n_g n_u | V^*_{pE_f}(E\mathbf{1} - \mathscr{H})^{-1}_{pq} V_{qE} | 0,0 \rangle. \tag{14}$$

To avoid confusion we shall always write $T_{pq}(E)$ and T_{pq} to indicate that the definitions (14) and (11b), respectively, hold. The cross sections now take on the appearance

$$\sigma(E;n_u \text{ even}) = \frac{\pi}{2E}(|T_{11}(E)|^2 + |T_{22}(E)|^2), \tag{15a}$$

$$\sigma(E;n_u \text{ odd}) = \frac{\pi}{2E}(|T_{12}(E)|^2 + |T_{21}(E)|^2). \tag{15b}$$

The expressions (15) for the cross sections are particularly simple, since mixed terms do not appear. The scattering process may be viewed as the incoherent superposition of two "scattering processes". For n_u being an even number, for instance, $|T_{pp}(E)|^2$ describes that the incoming electron first hops into the discrete state $|d_p\rangle$ and the outgoing electron leaves the molecule from the same state. Of course, during the scattering process the electron has visited both discrete states. We may thus introduce the partial integral cross sections

$$\sigma_{pq}(E) = \frac{\pi}{2E}|T_{pq}(E)|^2 \tag{16}$$

and consider the continua coupled to the respective discrete states as quasiscattering channels.

Under certain conditions the differential cross sections (12) can be related to the integral cross sections (15). In the case of a single discrete state it is known[38–40] that for scattering in a single partial wave, the differential cross section can be expressed as the product of an energy-independent angular factor and the integral cross section. If in the absence of vibronic coupling the scattering is dominated by a single partial wave for each discrete state, we may derive analogous relations which hold in the presence of vibronic coupling. For the excitation of an odd number of nontotally symmetric quanta the result is particularly simple and reads

$$\left(\frac{d\sigma}{d\Omega}\right)_{n_u\text{odd}} = f(\theta)[\sigma_{12}(E) + \sigma_{21}(E)] + f_{12}(\theta)\frac{\pi}{2E}[T_{12}(E)T^*_{21}(E) + T^*_{12}(E)T_{21}(E)], \tag{17a}$$

where θ is the scattering angle. The angular factors $f(\theta)$ and $f_{12}(\theta)$ are given in Appendix A. The analogous result for n_u being an even number is

$$\left(\frac{d\sigma}{d\Omega}\right)_{n_u\text{even}} = g_{11}(\theta)\sigma_{11}(E) + g_{22}(\theta)\sigma_{22}(E) + g_{12}(\theta)\frac{\pi}{2E}[T_{11}(E)T^*_{22}(E) + T^*_{11}(E)T_{22}(E)]. \tag{17b}$$

The angular factors $g_{11}(\theta)$, $g_{22}(\theta)$, and $g_{12}(\theta)$ are also given in Appendix A. $g_{11}(\theta)$ and $g_{22}(\theta)$ are the same as those derived for single discrete states.[38–40] In contrast to Eq. (12), the differential cross sections (17) are averaged over the orientations of the molecular target.

According to Eqs. (15)–(17) the angular dependence of the differential cross sections varies with the total energy E. The factors $f(\theta)$, $g_{11}(\theta)$, and $g_{22}(\theta)$ are symmetric functions with respect to $\theta = \pi/2$. The angular factors $f_{12}(\theta)$ and $g_{12}(\theta)$, on the other hand, are antisymmetric about $\theta = \pi/2$. Of course, all angular factors and thus the differential cross sections are periodic functions with period π. In the presence of a single resonance only, the angular part of the cross sections does not depend on the energy and is symmetric about $\theta = \pi/2$. Hence, a strong dependence on energy and an asymmetric shape of the differential cross sections are indications for the presence of two or more resonances. The appearance of odd quanta of nontotally symmetric modes implies, furthermore, that the vibronic coupling mechanism is active in these resonances.

III. LOCAL APPROXIMATIONS

In the preceding section the general theory of nuclear dynamics in vibronically coupled resonance states has been discussed. The nuclear motion is found to be governed by an effective, complex, energy-dependent, and nonlocal matrix potential. Although the relevant working equations are of simple structure, explicit computations for realistic systems with such an effective Hamiltonian are extremely tedious. As usually done in the simpler case of a single resonance state, we discuss in the following a few approximations which, in general, simplify the computational procedure and allow for the interpretation of the results which is difficult otherwise. These approximations have in common that the nonlocal Hamiltonian is replaced by a local Hamiltonian. The *fixed-nuclei* limit, $T_N \to 0$, is a convenient starting point for the discussion of local approximations. In this limit the

This article is copyrighted as indicated in the article. Reuse of AIP content is subject to the terms at: http://scitation.aip.org/termsconditions. Downloaded to IP: 130.89.98.137 On: Sun, 30 Nov 2014 02:07:35

theory is particularly transparent and contact can be made with fixed-nuclei electronic *ab initio* calculations.

A. The fixed-nuclei limit

In the fixed-nuclei limit the operator $E - \tilde{H}_0$ appearing in the argument of the level-shift operator in Eq. (8) reduces to

$$E' = E - V_0(\mathbf{Q}). \tag{18}$$

For a fixed total energy of the system, E' is the kinetic energy of the electron and is a function of the internuclear distances because the threshold itself has become a function of these distances.

Considering a single resonance state, the scattering cross section in the fixed-nuclei limit takes on the appearance similar to the standard Breit–Wigner formula[41]

$$\sigma(E') = \frac{\pi}{2E'}|T(E')|^2 = \frac{2\pi}{E'}\frac{[\Gamma(E')/2]^2}{[E' - \epsilon(\mathbf{Q}) - \Delta(E')]^2 + [\Gamma(E')/2]^2}. \tag{19}$$

$\epsilon(\mathbf{Q})$ is the energy of the discrete state relative to threshold and $\Delta - i\Gamma/2$ is the level-shift function for this state. We remind that this function depends also explicitly on $\mathbf{Q}$ as can be seen from Eq. (9). Another quantity of interest is the fixed-nuclei phase shift $\delta(E')$ which can be obtained from the K "matrix" $K(E')$ according to

$$\operatorname{tg}\delta(E') = K(E') = -\frac{\Gamma(E')/2}{E' - \epsilon(\mathbf{Q}) - \Delta(E')}. \tag{20}$$

In the case of vibronically coupled resonances the resulting expressions for the fixed-nuclei electron–molecule scattering cross section and the corresponding phase shift are more complicated than for a single resonance. These expressions can be obtained from the working equations of the preceding section. To introduce the fixed-nuclei limit for vibronically coupled resonances, it is convenient to rewrite Eqs. (14)–(16). We define a matrix $\mathbf{T}(E)$,

$$\mathbf{T}(E) = \begin{pmatrix} T_{11}(E) & T_{12}(E) \\ T_{21}(E) & T_{22}(E) \end{pmatrix} \tag{21}$$

which allows the evaluation of the cross section according to

$$\sigma(E) = \frac{\pi}{2E}\mathrm{Tr}[\mathbf{T}^\dagger(E)\mathbf{T}(E)], \tag{22}$$

where $\mathrm{Tr}(\mathbf{A})$ is the trace of $\mathbf{A}$. The K matrix corresponding to $\mathbf{T}(E)$ is defined as usual[41] (apart from a factor π)

$$\mathbf{K}(E) = -\mathbf{T}(E)[1 - i\,\mathbf{T}(E)]^{-1}. \tag{23}$$

The fixed-nuclei limit is obtained if E is replaced by E' defined in Eq. (18) and the elements $T_{pq}(E')$, $p,q = 1,2$, are defined by

$$T_{pq}(E') = [\Gamma_{pp}(E')]^{1/2}[E'\mathbf{1} - \mathscr{H}_{\mathrm{FN}}(E')]^{-1}_{pq}[\Gamma_{qq}(E')]^{1/2}, \tag{24a}$$

$$\mathscr{H}_{\mathrm{FN}} = \begin{pmatrix} V_1 + F_{11}(E') & F_{12}(E') + U_{12} \\ F_{21}(E') + U_{12} & V_2 + F_{22}(E') \end{pmatrix}, \tag{24b}$$

where $F_{pq}(E')$ is the fixed-nuclei level-shift function, see Eq. (9).

The fixed-nuclei K matrix corresponding to the exact K matrix in Eq. (23) reads

$$\mathbf{K}(E') = -\frac{1}{(A_1A_2 - U_{12}^2)} \times \begin{pmatrix} A_2\Gamma_{11} & -U_{12}[\Gamma_{11}\Gamma_{22}]^{1/2} \\ -U_{12}[\Gamma_{11}\Gamma_{22}]^{1/2} & A_1\Gamma_{22} \end{pmatrix}, \tag{25a}$$

$$A_p = E' - \epsilon_p(\mathbf{Q}) - \Delta_{pp}(E'); \quad p = 1,2. \tag{25b}$$

It should be remembered that $\epsilon_p = V_p - V_0$ is the energy of the discrete state $|d_p\rangle$ relative to the threshold V_0 which is the potential energy surface of the target. The cross section is now obtained from

$$\sigma(E') = \frac{2\pi}{E'}\sum_i \sin^2\delta_i(E'), \tag{26}$$

where the phase shifts are related to the eigenvalues $K_\pm(E')$ of $\mathbf{K}(E')$ by

$$\operatorname{tg}\delta_\pm(E') = K_\pm(E'). \tag{27}$$

Neglecting vibronic coupling in the resonance states, i.e., $U_{12} = 0$, the matrix $\mathbf{K}(E')$ becomes diagonal and we recover Eq. (20) for a single resonance state.

In the presence of a single resonance and for weakly energy-dependent level-shift functions, the K matrix (20) possesses only one pole. Indeed, this pole is commonly used to define the potential energy curve of the resonance.[26,30,31,42] In the present case of two resonances the K matrix Eq. (25) exhibits two poles which can be used to define potential energy curves for these resonances. These poles are obtained as the zeros of $A_1A_2 - U_{12}^2$. We may write

$$A_1A_2 - U_{12}^2 = [E' - W_+(E')][E' - W_-(E')], \tag{28a}$$

where the new quantities

$$2W_\pm = \epsilon_1 + \Delta_{11} + \epsilon_2 + \Delta_{22} \pm [(\epsilon_1 + \Delta_1 - \epsilon_2 - \Delta_2)^2] + 4U_{12}^{1/2} \tag{28b}$$

help to express the phase shift as

$$\operatorname{tg}\delta_\pm(E') = -\frac{\Gamma_\pm}{2}\left[\frac{1}{E' - \mathbf{W}_+} - \frac{1}{E' - \mathbf{W}_-}\right], \tag{29a}$$

$$\Gamma_\pm(E') = \{\Gamma_{11}A_2 + \Gamma_{22}A_1 \pm [(\Gamma_{11}A_2 - \Gamma_{22}A_1)^2 + 4\Gamma_{11}\Gamma_{22}U_{12}^2]^{1/2}\}/2(W_+ - W_-). \tag{29b}$$

As discussed in the preceding section, the interaction of the discrete states with the continuum gives rise to the level-shift functions $F_{pp} = \Delta_{pp} - i\Gamma_{pp}/2$. The index p, which takes on the values 1 and 2, characterizes the discrete states which are *diabatic* states. The nuclear motion in the diabatic resonance which has developed from the discrete state $|d_p\rangle$ is governed by the effective potential $V_p + \Delta_{pp} - i\Gamma_{pp}/2$. In the present section we have diagonalized the matrix K, Eq. (25), and thus obtained the quantities

$$V_0 + W_\pm(E') - i\Gamma_\pm(E')/2$$

which, in analogy to the single-resonance case, can be viewed as the effective potentials describing the nuclear motion in the *adiabatic* resonances. From Eq. (29) we see that both adiabatic resonances contribute to the phase shifts δ_+ and δ_-. It will become clear in Sec. III B that this is due to the dependence of the effective potentials on the energy.

This article is copyrighted as indicated in the article. Reuse of AIP content is subject to the terms at: http://scitation.aip.org/termsconditions. Downloaded to IP: 130.89.98.137 On: Sun, 30 Nov 2014 02:07:35

B. Local potentials

The energy dependence of the level-shift functions $F_{pq}(E')$ complicates the calculations of the cross sections. In the presence of a single resonance it has been shown[43] that a complex potential which depends solely on the nuclear coordinates may explain the experimental observations in some cases. This model has been termed the *boomerang* model.[43] We, therefore, extend this model to the present situation of vibronically coupled resonances. The elimination of the energy dependence of F_{pq} is achieved by the Breit–Wigner approximation.[41,44] However, this approximation is not unique and may lead to different local potentials.[45]

Here we follow the most widely used local approximations[25–31,42] obtained by replacing $F_{pq}(E')$ by their values at the resonance energy which is defined by the pole of the fixed-nuclei K matrix. For a single resonance this energy is determined via Eq. (20),

$$E'(\mathbf{Q}) - \epsilon(\mathbf{Q}) - \Delta[E'(\mathbf{Q})] = 0. \tag{30a}$$

$E'(\mathbf{Q})$ is now a function of the nuclear coordinates and the width $\Gamma[E'(\mathbf{Q})]$ and shift $\Delta[E'(\mathbf{Q})]$ become functions of these coordinates only. We denote these energy independent functions by $\Gamma(\mathbf{Q})$ and $\Delta(\mathbf{Q})$, respectively. In the case of two resonances, the fixed-nuclei K matrix (25) exhibits two poles giving rise to two resonance energies $W_+(\mathbf{Q})$ and $W_-(\mathbf{Q})$. These are determined via

$$E'(\mathbf{Q}) - W_\pm[E'(\mathbf{Q})] = 0, \tag{30b}$$

where $W_\pm(E')$ have been given in Eq. (28).

By noting that $A_1A_2 - U_{12}^2$ in Eq. (28a) vanishes at $E' = W_\pm(\mathbf{Q})$, we easily obtain the following expressions for the phase shifts in the local approximation

$$\operatorname{tn}\delta_\pm(E') = -\frac{\Gamma_\pm(\mathbf{Q})/2}{E' - W_\pm(\mathbf{Q})}. \tag{31a}$$

In contrast to the original expression (29) for the phase shifts where both $W_+(E')$ and $W_-(E')$ have been seen to contribute, only a single resonance energy contributes to a phase shift in the local approximation. The situation is now very similar to that encountered in the case of noninteracting resonances, except that this interaction is implicitly taken into account in $\Gamma_\pm$ and $W_\pm$. We may thus identify $\Gamma_\pm(\mathbf{Q})$ with the widths corresponding to the energies $W_\pm(\mathbf{Q})$. From Eq. (29b) one finds

$$\Gamma_\pm(\mathbf{Q}) = |\Gamma_{11}[W_\pm(\mathbf{Q})]A_2[W_\pm(\mathbf{Q})] + \Gamma_{22}[W_\pm(\mathbf{Q})]A_1[W_\pm(\mathbf{Q})]|/[W_+(\mathbf{Q}) - W_-(\mathbf{Q})]. \tag{31b}$$

The local, energy independent effective potential needed to compute the vibrational excitation cross sections cannot be obtained in analogy to the single resonance case by replacing E' in the energy dependent potential by $E'(\mathbf{Q})$. Two solutions of Eq. (30b) are available and it is not clear how the replacement should be performed in the working equations. This difficulty arises because the Hamiltonian $\mathscr{H}$ is in the diabatic representation and $W_\pm(\mathbf{Q})$ are the *adiabatic resonance energies*. $W_+(\mathbf{Q})$ and $W_-(\mathbf{Q})$ do not arise naturally as the eigenvalues of a *single* Hermitian matrix. There are infinitely many ways to construct Hermitian matrices with $W_\pm(\mathbf{Q})$ as eigenvalues all differing by a unitary transformation. This contrasts the situation encountered for noninteracting resonances, where the diabatic and adiabatic representations are equivalent and unique. The problem can be partially solved by considering $W_\pm(\mathbf{Q}) - i\Gamma_\pm(\mathbf{Q})/2$ as the potentials controlling the nuclear dynamics in the adiabatic resonances which are assumed not to interact with each other. This procedure is useful in those cases where nonadiabatic effects are small (see Sec. III C).

To avoid the abovementioned difficulty one can alternatively introduce the *diabatic resonance energies* by solving two equations of the type (30a), one for each diabatic resonance, and subsequently insert the solutions $E_1'(\mathbf{Q})$ and $E_2'(\mathbf{Q})$,

$$E_p'(\mathbf{Q}) - \epsilon_p(\mathbf{Q}) - \Delta_{pp}[E_p'(\mathbf{Q})] = 0; \quad p = 1,2 \tag{32}$$

into the level-shift functions $F_{11}(E')$ and $F_{22}(E')$, respectively, or, more precisely, into the matrix elements $V_{1E'}$ and $V_{2E'}$. In particular, the Hamiltonian $\mathscr{H}_{\mathrm{FN}}(E')$ introduced in Eq. (24) is replaced in a unique way by a Q-dependent Hamiltonian, which we denote by $\mathscr{H}_{\mathrm{FN}}(\mathbf{Q})$. After these replacements of energy dependent quantities by energy independent ones, the following expression for the T matrix can be used to evaluate the cross sections

$$\mathbf{T}(E) = \langle \mathbf{n}| \begin{pmatrix} V^*_{1E_f} & 0 \\ 0 & V^*_{2E_f} \end{pmatrix} [E\mathbf{1} - T_N\mathbf{1} - \mathscr{H}_{\mathrm{FN}}(\mathbf{Q})]^{-1} \times \begin{pmatrix} V_{1E_i} & 0 \\ 0 & V_{2E_i} \end{pmatrix} |\mathbf{0}\rangle. \tag{33}$$

Note that $\Gamma_{pq}(E) = V^*_{pE}V_{qE}$. In principle one may also replace the entry and exit amplitudes[40] V_{pE_i} and V_{pE_f} in Eq. (33) by the corresponding energy independent quantities.

This approach via diabatic resonance energies should be particularly useful if the level-shift functions depend only weakly on the energy or if the coupling element U_{12} is small. In other cases it could be of advantage to proceed via the adiabatic resonance energies.

C. The adiabatic approximation

In optical spectroscopy of bound electronic states and in other related fields the so-called Franck–Condon and adiabatic approximations are commonly used.[46] The adiabatic potential energy surfaces are calculated and subsequently the nuclear motion is determined independently for each electronic state. The same procedure could also be useful in the case of resonance states. To keep the discussion short we follow here Ref. (36) which treats the analogous electronic bound state problem and refer to this reference for more details.

Our starting point is expression (33) for the T matrix in which $\mathscr{H}_{\mathrm{FN}}(\mathbf{Q})$ is the effective potential describing the nuclear motion in the coupled resonance states. The eigenvalues $V_\pm$ of the effective potential are obtained using the eigenvector matrix $\mathbf{S}(\mathbf{Q})$ according to

$$\mathbf{V}(\mathbf{Q}) = \mathbf{S}(\mathbf{Q})\mathscr{H}_{\mathrm{FN}}(\mathbf{Q})\mathbf{S}^t(\mathbf{Q}) = \begin{pmatrix} V_+(\mathbf{Q}) & 0 \\ 0 & V_-(\mathbf{Q}) \end{pmatrix}, \tag{34a}$$

$$2V_\pm = V_1 + F_{11} + V_2 + F_{22} \pm [(V_1 + F_{11} - V_2 - F_{22})^2 + 4(U_{12} + F_{12})^2]^{1/2} \tag{34b}$$

where the superscript "t" indicates the operation "trans-

This article is copyrighted as indicated in the article. Reuse of AIP content is subject to the terms at: http://scitation.aip.org/termsconditions. Downloaded to IP: 130.89.98.137 On: Sun, 30 Nov 2014 02:07:35

pose". Care must be taken at degeneracies $V_+ = V_-$ at which $\mathbf{S}\,\mathbf{S}' = \mathbf{1}$ might not be valid. The eigenvalues V_+ and V_- are functions of the nuclear coordinates and can be considered as the *adiabatic* potential energy surfaces of the adiabatic resonances. In contrast to the bound state problem, these surfaces are complex. The nuclear motion on these surfaces is thus more complicated in the case of resonances than for bound states.

Since the eigenvector matrix $\mathbf{S}$ depends on the nuclear coordinates, this matrix does not commute with the nuclear kinetic energy operator T_N appearing in Eq. (33). In complete analogy to the situation found for bound states, the transformed Hamiltonian reads

$$\mathscr{H}' \equiv \mathbf{S}[T_N\mathbf{1} + \mathscr{H}_{\rm FN}(\mathbf{Q})]\mathbf{S}' = T_N\mathbf{1} + \mathbf{V} - \mathbf{\Lambda}. \tag{35}$$

In addition to the adiabatic potential energy surfaces there appears in the Hamiltonian $\mathscr{H}'$ a nondiagonal matrix operator $\mathbf{\Lambda}$. The nondiagonal term Λ_{12} depends on the nuclear momenta and couples the nuclear motions in the adiabatic resonances. The *nonadiabatic operator* $\mathbf{\Lambda}$–as we shall call it–is neglected in the adiabatic approximation. For vibronically coupled bound states its behavior as a function of the nuclear coordinates gives much information on the validity of the adiabatic approximation. Its investigation should also be helpful in the understanding of the nuclear dynamics in resonances. Here, the additional complication arises that the nonadiabatic operator is complex. The explicit expressions for the elements of $\mathbf{\Lambda}$ are very similar to those given in Ref. 36 for bound states and are not repeated here. We shall rather discuss these elements in Sec. IV in the context of an explicit example pointing out the major differences between bound and resonance states.

In the adiabatic approximation the nonadiabatic operator $\mathbf{\Lambda}$ is neglected and *each* element $T_{pq}(E)$ of the scattering T matrix (33) reduces to

$$T_{\rm ad}(E) = T_+(E) + T_-(E), \tag{36a}$$

$$T_\pm(E) = \langle \mathbf{n}|X_{f\pm}\,[E - T_N - V_\pm\,]^{-1}X_{i\pm}\,|\mathbf{0}\rangle, \tag{36b}$$

where X_{i+} and X_{i-} are given by $S_{1q}V_{qE_i}$ and $S_{2q}V_{qE_i}$, respectively, for any element $T_{pq}(E)$, and X_{f+} and X_{f-} are defined analogously. It is seen that the T matrix in the adiabatic approximation decouples into two individual T matrices T_+ and T_-. Each of T_+ and T_- describes the scattering via a single adiabatic resonance, the nuclear motion in this resonance being governed by the complex potential energy surface V_+ and V_-, respectively. We may thus treat the resonances separately in the adiabatic approximation. In order to compute the scattering cross sections we must superpose T_+ and T_- according to the general formulas (15)–(17). This gives rise to interference effects.

In optical spectroscopy the so-called Franck–Condon approximation is widely used. This approximation can be determined by starting from the adiabatic approximation and neglecting the dependence of optical transition matrix elements on the nuclear coordinates. For resonance states we may use the same procedure and consider the quantities $X_{f\pm}$ and $X_{i\pm}$ in Eq. (36) to be independent of $\mathbf{Q}$. It is convenient to define these Q-independent quantities by evaluating them at some reference geometry $\mathbf{Q}_0$, which is usually the equilibrium geometry of the target. Consequently, the T matrix in the Franck–Condon approximation reads ($p = 1,2$)

$$(T_{\rm FC})_{pp} = V^*_{pE_f}\langle \mathbf{n}|\,[E - T_N - V_\pm\,]^{-1}|\mathbf{0}\rangle V_{pE_i}, \tag{37a}$$

$$(T_{\rm FC})_{pq} = 0 \quad \text{for } p \neq q. \tag{37b}$$

Whether V_+ or V_- appears in Eq. (37a) for a given index p depends on the discrete state $|d_p\rangle$ from which this adiabatic potential energy surface originates. Interestingly, T_{12} and T_{21} vanish in the Franck–Condon approximation implying, via Eq. (15), that an *odd* number of quanta of nontotally symmetric vibrational modes *cannot* be excited in this approximation. The same situation is encountered in the treatment of bound states.[37,46]

IV. MODEL EXAMPLES OF NUCLEAR DYNAMICS IN INTERACTING RESONANCES

Numerical nonlocal calculations of the nuclear dynamics in vibronically coupled resonances are prohibitively difficult for realistic systems. Even in the case of a single resonance state, complete nonlocal calculations are hardly available. They exist for the nitrogen molecule,[49] the hydrogen molecule,[50] and a nearly complete nonlocal calculation also for the fluorine molecule.[51] If two or more nuclear coordinates are involved, as is expected for polyatomic molecules, the computation is extremely tedious even for an isolated resonance. Making use of local approximations reduces considerably the numerical effort, but the computations are still cumbersome for real polyatomic molecules and are beyond the scope of this paper.

Nevertheless, we are interested in investigating possible dynamical effects due to vibronic coupling, which can be done by resorting to models. In this way we may not reproduce or predict the details of experimental observations, but rather aim at the general aspects of the possible phenomena. We have a particular model in mind which has been successful in the case of vibronic coupling in bound states.[36,52,53] To be specific we consider here two discrete states of different symmetry coupled by a nondegenerate nontotally symmetric vibrational mode described by the normal coordinate Q_u. Furthermore, we include the action of a totally symmetric mode with the normal coordinate Q_g. For this situation Eqs. (15)–(17) apply. The model now consists of the following effective Hamiltonian:

$$\mathscr{H} = \tilde{H}_0\mathbf{1} + \begin{pmatrix} E_1 + \kappa_1 Q_g + F_{11}(E - \tilde{H}_0) & \lambda Q_u \\ \lambda Q_u & E_2 + \kappa_2 Q_g + F_{22}(E - \tilde{H}_0) \end{pmatrix}, \tag{38}$$

where the nomenclature of Ref. 36 is used. Comparing with the general expression (8) we note that the discrete-state quantities $V_1 - V_0$, $V_2 - V_0$, and U_{12} have been expanded about $Q_0 = 0$ in powers of Q_g and Q_u up to the linear term. E_1 and E_2 are the vertical energy differences at Q_0 between the target potential energy surface and the corresponding diabatic surfaces of the discrete states $|d_1\rangle$ and $|d_2\rangle$, respectively. The quantities κ_1, κ_2, and λ are called *intra-* and *interstate coupling constants*.[36]

The target system is taken to be a two dimensional harmonic oscillator, i.e., $\tilde{H}_0$ takes on the appearance

$$\tilde{H}_0 = T_N + V_0, \tag{39a}$$

This article is copyrighted as indicated in the article. Reuse of AIP content is subject to the terms at: http://scitation.aip.org/termsconditions. Downloaded to IP: 130.89.98.137 On: Sun, 30 Nov 2014 02:07:35

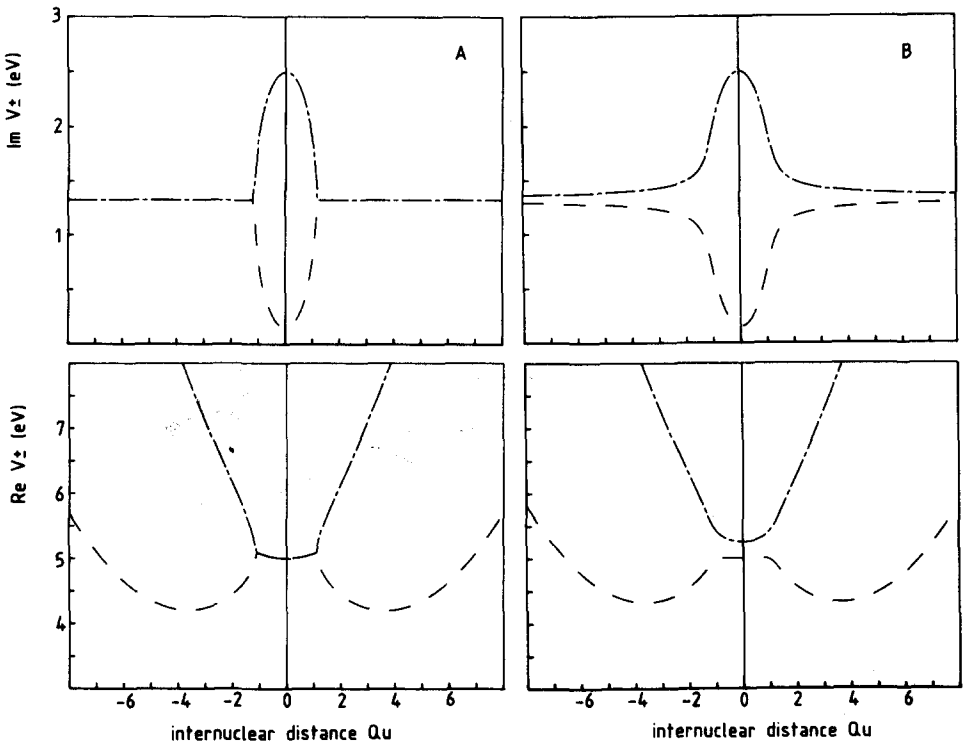

FIG. 1. Adiabatic potential energy curves of the square-root intersection model along the nontotally symmetric coordinate Q_u for two characteristic values of the Q_g coordinates. *Left side* (1A): Q_g is chosen at the intersection, i.e., $Q_g = Q_g^c$. *Right side* (1B): Q_g is chosen such that the energy difference at $Q_u = 0$ is 0.25 eV. The relevant parameters are $\lambda = 1.1$, $\Gamma_{11} = 0.25$, $\Gamma_{22} = 2.5$, and $\omega_u = 0.15$, all in eV.

$$T_N = -\tfrac{1}{2}\omega_g \frac{\partial^2}{\partial Q_g^2} - \tfrac{1}{2}\omega_u \frac{\partial^2}{\partial Q_u^2}, \tag{39b}$$

$$V_0 = \tfrac{1}{2}\omega_g Q_g^2 + \tfrac{1}{2}\omega_u Q_u^2, \tag{39c}$$

where ω_g and ω_u are the vibrational frequencies of the totally symmetric and nontotally symmetric modes, respectively. The diabatic potential energy surfaces of the discrete states are thus shifted harmonic surfaces. These states are coupled to the continuum resulting in the nonlocal level-shift operators F_{11} and F_{22}, and to each other via the vibronic coupling term $U_{12} = \lambda Q_u$.

A. Static aspects of the model

As discussed above, the potential energy surfaces of the discrete states are harmonic surfaces shifted with respect to the target surfaces. Despite this simple structure of the diabatic surfaces, the adiabatic surfaces are of considerable complexity. Since the discrete states are of different symmetries, the adiabatic surfaces may cross at $Q_u = 0$. As soon as Q_u takes on values different from zero the adiabatic surfaces repel, giving rise to a *conical intersection*.[54–56] Conical intersections play an important role in the nuclear dynamics in bound electronic states of polyatomic molecules.[36] In the case of resonance states, the coupling to the continuum may considerably change the picture. The potential energy surfaces become complex functions of **Q**. In the following we briefly discuss within the present model the major differences between bound and resonance states. To keep the discussion as transparent as possible we put the widths Γ_{11} and Γ_{22} to be constants, i.e., independent of the energy and the nuclear coordinates.

In the bound state problem, i.e., $\Gamma_{11} = \Gamma_{22} = 0$, the adiabatic surfaces $V_+(Q_g,Q_u)$ and $V_-(Q_g,Q_u)$ exhibit a conical intersection at $Q_u^c = 0$ and $Q_g^c = (E_2 - E_1)/(\kappa_1 - \kappa_2)$. A perspective view of these surfaces for a prototype conical intersection can be seen in Fig. 6 of Ref. 36. In the present model these real surfaces are identical with the poles of the fixed-nuclei K matrix, W_+ and W_-, defined in Eq. (30b). We shall use this notation to distinguish between the complex and the corresponding real surfaces. In the resonance-state situation the surfaces $V_\pm$ are given by the eigenvalues of $\mathscr{H} - T_N\mathbf{1}$ and read

$$V_\pm(Q_g,Q_u) = V_0(Q_g,Q_u) + \{[Z_1 + Z_2] \pm [(Z_1 - Z_2)^2 + 4\lambda^2 Q_u^2]^{1/2}\}/2, \tag{40a}$$

$$Z_p(Q_g) = E_p + \kappa_p Q_g - i\Gamma_{pp}/2; \quad p = 1,2. \tag{40b}$$

Being complex, these surfaces may intersect at two points, the coordinates of which are given by

$$Q_u^\pm = \pm(\Gamma_{11} - \Gamma_{22})/4\lambda, \tag{41a}$$

$$Q_g^c = (E_2 - E_1)/(\kappa_1 - \kappa_2). \tag{41b}$$

The value of Q_g at these intersections is the same as for the conical intersection in the corresponding bound state problem obtained for vanishing widths. In Fig. 1A the surfaces $V_\pm$ are shown as a function of Q_u at $Q_g = Q_g^c$. The real and imaginary parts of the curves are shown separately. For values of Q_u between the degeneracy points Q_u^+ and Q_u^- the real parts, Re V_+ and Re V_-, are identical while the imaginary parts, Im V_+ and Im V_-, are not. These parts are identical everywhere else and the widths become $(\Gamma_{11} + \Gamma_{22})/2$. The two curves repel each other giving rise to an energy split

This article is copyrighted as indicated in the article. Reuse of AIP content is subject to the terms at: http://scitation.aip.org/termsconditions. Downloaded to IP: 130.89.98.137 On: Sun, 30 Nov 2014 02:07:35

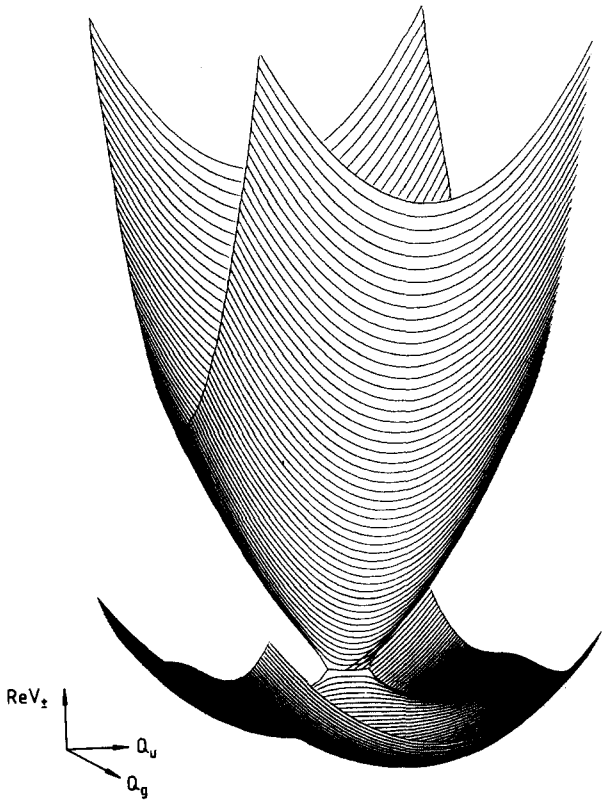

FIG. 2. Perspective view of the adiabatic energy surfaces of the square-root intersection model. Only the real parts of the surfaces are shown.

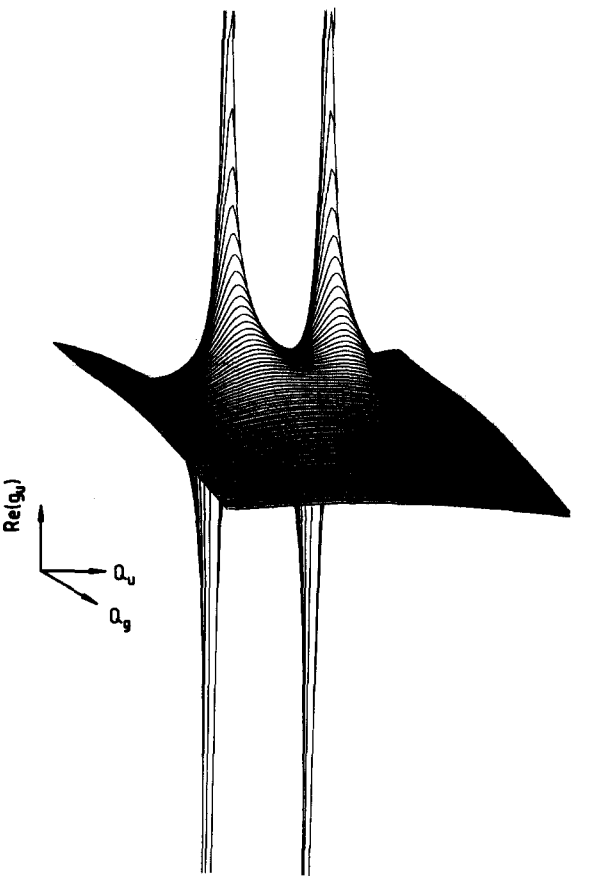

FIG. 3. Perspective view of the real part of the nonadiabatic coupling element g_u in the square-root intersection model.

$2\lambda\,[Q_u^2-(Q_u^{\pm})^2]^{1/2}$ compared to the split of $2\lambda Q_u$ in the bound state problem.

Figure 1B shows the surfaces $V_{\pm}$ as a function of Q_u for a value of Q_g which is different from Q_g^c. The degeneracies of Re V_+ and Re V_- and also of Im V_+ and Im V_- are lifted. For small values of $|Q_g-Q_g^c|$ the energies at the points (41) split proportionally to $[Q_g-Q_g^c]^{1/2}$, in contrast to a conical intersection situation, where the split is linear in $Q_g-Q_g^c$. The vicinity of the intersection of V_+ and V_- is thus characterized by the square roots of $Q_g-Q_g^c$ and $Q_u-Q_u^{\pm}$ along the Q_g and Q_u coordinates, respectively. This "square-root intersection", as we call it, is typical for complex surfaces. A perspective view of the real part of the surfaces V_+ and V_- is given in Fig. 2 for a square-root intersection situation. The types of intersections typical for bound state potential energy surfaces are discussed in Ref. 56.

The existence of two intersection points of V_+ and V_- gives rise to another interesting difference between the real parts of these functions and $W_{\pm}$. In a conical intersection situation, W_+ exhibits as a function of Q_u a single minimum at $Q_u=0$. W_- possesses a maximum at this point, but may show *two* minima at $Q_u\neq 0$. The condition for this symmetry breaking is

$$|2\lambda^2/\omega_u(E_1+\kappa_1 Q_g-E_2-\kappa_2 Q_g)|>1.$$

The symmetry breaking by a nontotally symmetric coupling mode is a well-known phenomenon for bound states.[57] As seen in Figs. 1 and 2, the real part of V_- may exhibit *three* minima, one at $Q_u=0$ and two at $Q_u\neq 0$. The minimum of V_- at $Q_u=0$ has its origin in the fact that for $Q_g=Q_g^c$, the curves Re V_+ and Re V_- are parallel to the target surface V_0 for values of Q_u between Q_u^- and Q_u^+. It is worth noting that the two minima at $Q_u\neq 0$ may energetically lie above or below the one at $Q_u=0$.

In the bound state situation, the nuclear motions on the adiabatic potential energy surfaces W_+ and W_- are coupled by a nonadiabatic operator. This coupling is singular at the conical intersection.[36] In the present resonance model, the nonadiabatic operator, defined via Eq. (35), reads

$$\Lambda=-\sum_{\alpha=g,u}\frac{\omega_\alpha}{2}\times\begin{pmatrix} g_\alpha^2 & -\dfrac{\partial g_\alpha}{\partial Q_\alpha}-2g_\alpha\dfrac{\partial}{\partial Q_\alpha}\\ \dfrac{\partial g_\alpha}{\partial Q_\alpha}+2g_\alpha\dfrac{\partial}{\partial Q_\alpha} & g_\alpha^2\end{pmatrix}, \tag{42a}$$

$$g_g=\frac{-(\kappa_1+\kappa_2)\lambda Q_u}{(Z_1-Z_2)^2+4\lambda^2 Q_u^2}, \tag{42b}$$

$$g_u=\frac{(Z_1-Z_2)\lambda}{(Z_1-Z_2)^2+4\lambda^2 Q_u^2}. \tag{42c}$$

As an example the real part of the element g_u is depicted in Fig. 3 for a prototype square-root intersection. Both complex elements g_u and g_g exhibit two singularities at the intersection points given by Eq. (41). The element g_g vanishes at

This article is copyrighted as indicated in the article. Reuse of AIP content is subject to the terms at: http://scitation.aip.org/termsconditions. Downloaded to IP: 130.89.98.137 On: Sun, 30 Nov 2014 02:07:35

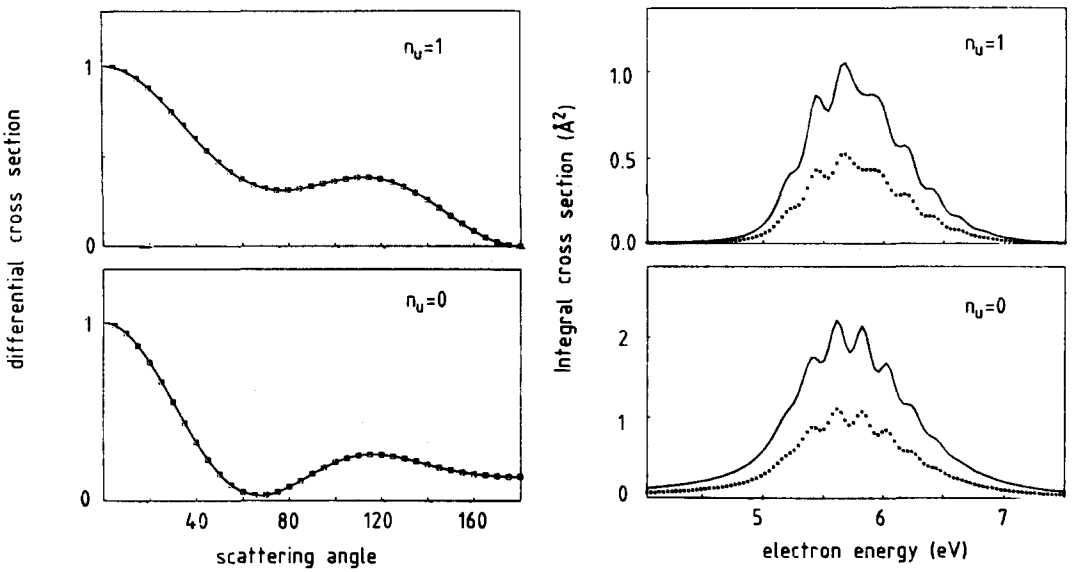

FIG. 4. Integral and differential resonant cross sections for the elastic channel $n_u = 0 \rightarrow 0$ and first vibrationally inelastic channel $n_u = 0 \rightarrow 1$. The differential cross sections are normalized to unity at the scattering angle $\theta = 0°$. The partial cross sections $\sigma_{11}(E) = \sigma_{22}(E)$ and $\sigma_{21}(E) = \sigma_{12}(E)$ are shown as broken lines for the elastic and inelastic channels, respectively. The relevant parameters are: $E_1 = E_2 = 5.85$, $\Gamma_{11} = \Gamma_{22} = 0.25$, $\lambda = 0.5$, and $\omega_u = 0.2$, all values in eV.

$Q_u = 0$ where $|g_u|$ takes on its minimum for fixed values of Q_g in the vicinity of Q_g^c. When $|\Gamma_{11} - \Gamma_{22}|$ grows, the intersection points around which the elements g_g and g_u are substantial move away from $Q_u = 0$. This weakens the nonadiabatic effects, at least those present in the elastic scattering, since the ground vibrational state of the target molecule is localized at $Q_u = 0$.

B. Numerical investigation of the nuclear dynamics

In this subsection we discuss integral and differential cross sections computed using the effective model Hamiltonian (38). Although this Hamiltonian is of simple structure, the numerical evaluation of the cross sections requires considerable effort. Assuming the hopping matrix elements V_{1E} and V_{2E} to solely depend on energy, the expressions for the cross sections simplify somewhat and read ($p,q = 1,2$)

$$\sigma_{pq}(E) = \frac{\pi}{2E}\Gamma_{pp}(E_f)\Gamma_{qq}(E_i)|\langle \mathbf{n}|R_{pq}|\mathbf{0}\rangle|^2, \tag{43}$$

where R_{pq} is the p,q element of the resolvent $(E\mathbf{1} - \mathscr{H})^{-1}$. Since the Hamiltonian describes linear vibronic coupling, the vibrational matrix elements of the resolvent can be calculated by continued fraction methods.[47,48,58] The evaluation of these elements is described in Appendix B.

We have performed numerous computations of the vibrational excitation cross sections for various values of the parameters appearing in the Hamiltonian (38). The results obtained exhibit several interesting effects originating from the vibronic interaction of the resonances. Out of these results we discuss here a few examples which should help in identifying typical vibronic coupling effects. For the sake of transparency we begin with examples of single-mode dynamics, i.e., only the coupling mode Q_u is considered and the totally symmetric mode Q_g is discarded. Furthermore, we put the widths to be constants. In our first example we consider two discrete states with the same energy and identical coupling to the continuum, i.e., $E_1 = E_2$ and $\Gamma_{11} = \Gamma_{22}$. These states should interact through the nontotally symmetric mode Q_u. Short lived states which fulfill these conditions to a sufficiently high accuracy are, for instance, core hole states of symmetric polyatomic molecules like[59] CO_2. The problem is exactly solvable, since the effective Hamiltonian (38) can be explicitly diagonalized by a Q_u-independent orthogonal transformation. The result simply reads

$$\langle n_u|R_{pq}|0\rangle = \sum_{\tilde{m}} \frac{\langle n_u|\tilde{m}\rangle\langle\tilde{m}|0\rangle}{E - E_1 + \lambda^2/\omega_u - m\omega_u + i\Gamma_{11}/2}, \tag{44}$$

where $|\tilde{m}\rangle$ are the vibrational states of the harmonic oscillator shifted by λQ_u. Explicit expressions for the product of Franck–Condon factors $\langle n_u|\tilde{m}\rangle\langle\tilde{m}|0\rangle$ can easily be given, see, e.g. Ref. 60. It should be remembered that Eq. (44) holds for $p = q$ when n_u is an even number and for $p \neq q$ when n_u is odd.

The integral and differential cross sections obtained for the first example are exhibited in Fig. 4 for the elastic and the first inelastic channel. Shown are also the quantities $\sigma_{11}(E)$ and $\sigma_{12}(E)$ [see Eq. (16)]. The differential cross sections are normalized to unity at $\theta = 0$. These normalized differential cross sections do not depend on the energy E as can be readily anticipated by considering Eq. (44). The transformation leading to this equation tells us that the nuclear motion takes place on two decoupled shifted harmonic oscillators, one shifted by $+\lambda Q_u$ and the other by $-\lambda Q_u$. Consequently, $T_{12} = T_{21}$ and $T_{11} = T_{22}$ in every channel and according to Eq. (17) the normalized differential cross sections are given by

$$[f(\theta) + f_{12}(\theta)]/[f(0) + f_{12}(0)]$$

and

$$[g_{11}(\theta) + g_{22}(\theta) + 2g_{12}(\theta)]/[g_{11}(0) + g_{22}(0) + 2g_{12}(0)]$$

for an odd and even number of quanta, respectively.

Since $f(\theta)$, $g_{11}(\theta)$, and $g_{22}(\theta)$ are symmetric functions and $f_{12}(\theta)$ as well as $g_{12}(\theta)$ are antisymmetric functions of $\theta - \pi/2$, the differential cross sections shown in Fig. 4 are

This article is copyrighted as indicated in the article. Reuse of AIP content is subject to the terms at: http://scitation.aip.org/termsconditions. Downloaded to IP: 130.89.98.137 On: Sun, 30 Nov 2014 02:07:35

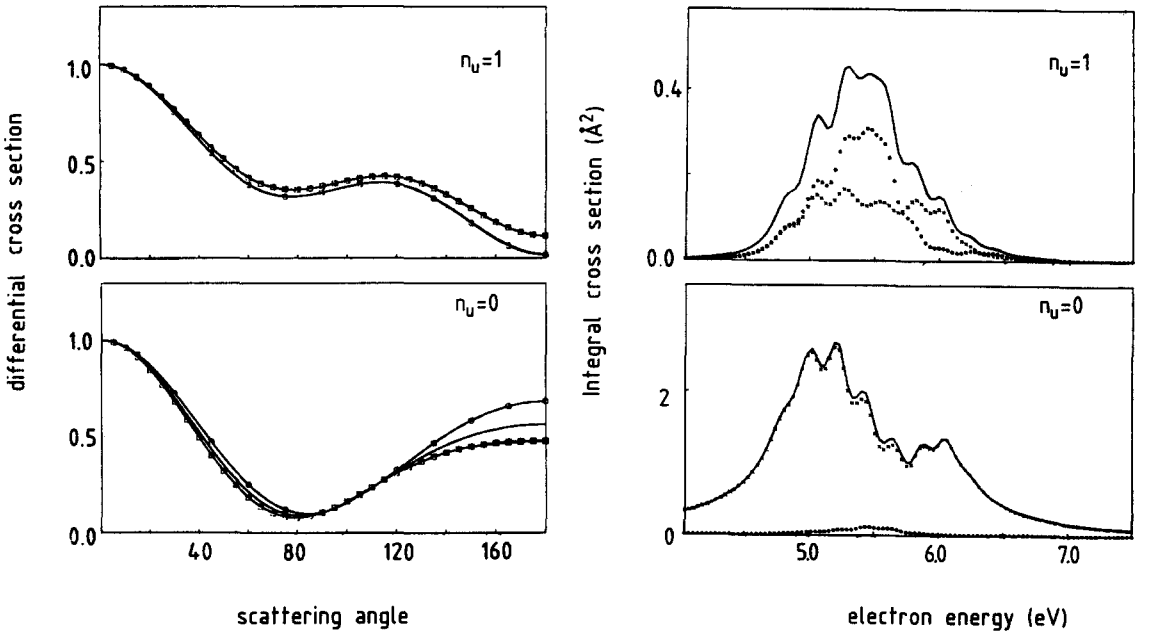

FIG. 5. Integral and differential resonant cross sections for the elastic channel $n_u = 0 \rightarrow 0$ and first vibrationally inelastic channel $n_u = 0 \rightarrow 1$. The differential cross sections are normalized to unity at the scattering angle $\theta = 0°$. They are shown for three values of the electron energy: $E = 5.3$ eV (solid curve), $E = 5.7$ eV (solid curve with squares), and $E = 6.5$ eV (solid curve with a few circles). Partial integral cross sections are also shown below the integral cross sections. $\sigma_{11}(E)$ and $\sigma_{21}(E)$ as circles and $\sigma_{22}(E)$ and $\sigma_{12}(E)$ as crosses. The values of the parameters are the same as in Fig. 4 except of $\Gamma_{11} = 0.05$ eV and $\Gamma_{22} = 0.45$ eV.

"maximally" nonsymmetric about $\theta = \pi/2$. In particular, $f(\theta) + f_{12}(\theta)$ vanishes at $\theta = \pi$ for all kinds of waves participating in the scattering. To draw Fig. 4 as well as in the following examples studied here we have chosen d waves and p waves to dominate the scattering associated with the discrete states $|d_1\rangle$ and $|d_2\rangle$, respectively. The corresponding angular factors are given in Table A1 of Appendix A for $l_1 = 2$, $m_1 = \pm 1$ and $l_2 = 1$, $m_2 = \pm 1$, respectively.

The parameters in our second example are the same as in the first example except that the widths of the two diabatic resonances are not equal. We have chosen $\Gamma_{11} = 0.05$ and $\Gamma_{22} = 0.45$ eV. Their mean value is the same as in the first example. The computed cross sections are displayed in Fig. 5. The elastic cross sections reflect the major differences between the two examples. For $\Delta\Gamma \neq 0$, where $\Delta\Gamma = \Gamma_{22} - \Gamma_{11}$, the elastic cross section is more asymmetric and exhibits two main humps. Particularly noticeable is the striking difference between the quantities $\sigma_{11}(E)$ and $\sigma_{22}(E)$ which are equal to each other in the first example where $\Delta\Gamma = 0$. In Fig. 5, $\sigma_{22}(E)$ dominates over $\sigma_{11}(E)$ which is noticeable only around the energy $E_{11} = E_{22}$ of the diabatic resonances. The ratio of σ_{11} and σ_{22} can partly be realized by considering the prefactors in Eq. (43) which are strongly in favor of σ_{22}. In spite of the smallness of $\sigma_{11}(E)$, the existence of two resonances has considerable impact on the asymmetry and energy dependence of the differential cross section.

For the excitation of an odd number of vibrational quanta the partial integral cross sections $\sigma_{12}(E)$ and $\sigma_{21}(E)$ also differ from each other. As can be seen in Fig. 5, both quantities are substantial. Consequently, the normalized differential cross section remains highly asymmetric about $\pi/2$ for most energies and is similar to that shown in Fig. 4. The most sensitive test for the underlying energy dependence is at $\theta = \pi$, where $d\sigma/d\Omega$ vanishes if $T_{12}(E) = T_{21}(E)$. It should be noticed that in the fixed-nuclei approximation we always find $T_{12}(E) = T_{21}(E)$ as can easily be anticipated from Eq. (24). For $\Delta\Gamma \neq 0$ the remarkable deviation of σ_{12} from σ_{21} changes strongly with energy E and is of dynamical origin and thus difficult to understand in simple terms. Instead of being equal, one rather finds

$$T_{12}(E + n\omega_u; n \rightarrow m) = T_{21}(E + m\omega_u; m \rightarrow n) \tag{45}$$

which implies that, apart from a shift of the energy axis, the cross sections for the vibrational excitations $n \rightarrow m$ and $m \rightarrow n$ are equal to each other for odd$|n - m|$. Note that E is the kinetic energy of the incident electron and $E + n\omega_u$ and $E + m\omega_u$ are total energies.

To gain some insight into the partial cross sections σ_{12} and σ_{21} we express them in terms of σ_{11} and σ_{22} for the elastic channel. These quantities possess counterparts in the spectroscopy of bound states and are thus simpler to rationalize. Using the basic relation (43) one obtains the following relation which is of relevance for small interstate coupling constant λ ($p \neq q$):

$$\sigma_{qp}(E; 0 \rightarrow 1) = \frac{2\lambda^2}{\Gamma_{11}\Gamma_{22}} L_q(E - \omega_u)\sigma_{pp}(E; 0 \rightarrow 0) + O(\lambda^4), \tag{46a}$$

where $L_q(E)$ is a Lorentzian given by

$$L_q(E) = [\Gamma_{qq}/2]^2 / \{[E - E_q]^2 + [\Gamma_{qq}/2]^2\}. \tag{46b}$$

In general, σ_{12} and σ_{21} for the first inelastic channel can only be substantial at energies where the elastic partial cross sections σ_{22} and σ_{11}, respectively, are not too small. This finding applies to Fig. 5 and in particular to Fig. 6 which shows the results of the next example. Following Eq. (46), the presence of a small width, say Γ_{11}, acts on σ_{22} as a "window" via the narrow Lorentzian L_1 giving rise to a sharp peak at $E \approx E_1 + \omega_u$. Such peaks have been observed in some of the

This article is copyrighted as indicated in the article. Reuse of AIP content is subject to the terms at: http://scitation.aip.org/termsconditions. Downloaded to IP: 130.89.98.137 On: Sun, 30 Nov 2014 02:07:35

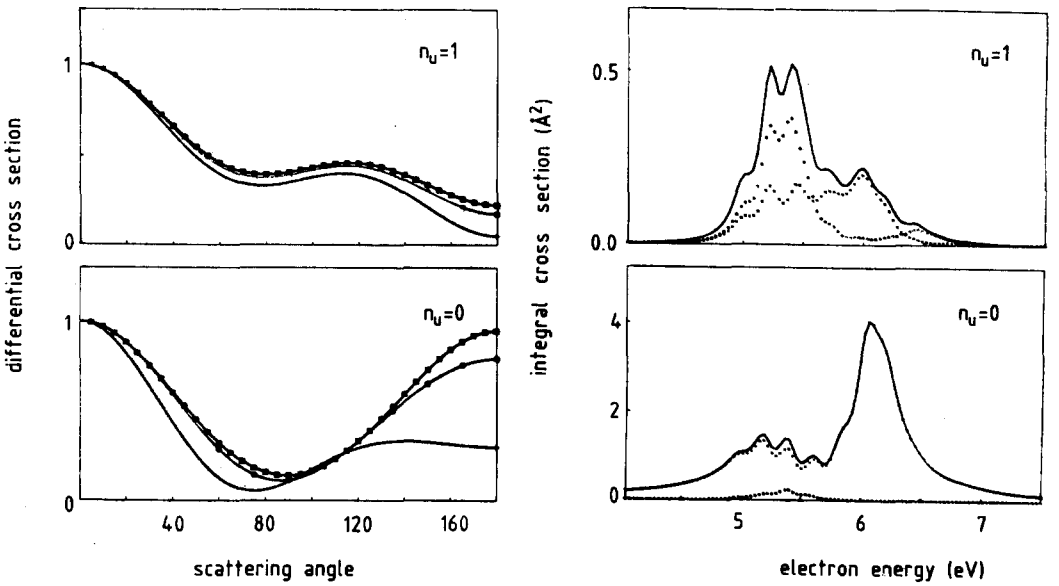

FIG. 6. Integral and differential resonant cross sections. For more details see Fig. 5. The values of the parameters are the same as in Fig. 5 except of $E_1 = 5.45$ eV and $E_2 = 5.85$ eV.

computed inelastic excitation functions. Of course, Eq. (46) only applies when λ is small or, more precisely, when $\sigma(E;0\rightarrow 2)$ can be neglected compared to $\sigma(E;0\rightarrow 0)$.

The results shown in Fig. 6 have been computed using the same parameters as used in the preceding example except that the diabatic state with the smaller width has been shifted downwards by $2\omega_u$: $E_2 = E_1 + 2\omega_u$. The major impact of this change of parameters on the cross sections is the remarkable increase of the weight of the second hump at about $E = 6$ eV. To explain this finding we resort to Fig. 1B which shows the adiabatic potential energy curves $V_\pm$ in a situation similar to the present one. Assuming the adiabatic approximation to apply (see Sec. III C), the real part of the "lower" curve, Re V_-, gives rise to the progression of peaks constituting the first hump in the (elastic) cross section of Fig. 6. The energy spacing of adjacent peaks is indeed $\approx\omega_u$ as expected in such a situation. The second hump corresponds to the real part of the "upper" curve Re V_+. This curve is steep and leads to large spacings of the energy levels. The substructure of the second hump is due to the nonadiabatic interaction of these levels with nearby lying levels of Re V_-. The situation in the preceding example, Fig. 5, is somewhat different. In this example the adiabatic potential curves V_+ and V_- are degenerate at two points as seen in Fig. 1A. The nonadiabatic matrix elements discussed in Sec. IV A diverge at these points and the adiabatic approximation fails completely. The cross sections resemble, therefore, those in our first example shown in Fig. 4, where a Q_u-independent transformation has lead to the exact solution of the problem, i.e., where the diabatic picture[61] and not the adiabatic one applies.

It is encouraging to see that the concepts of adiabatic potential energy curves widely used in spectroscopy of long-lived states are also useful in the context of scattering via resonance states. For a discussion of a related model in spectroscopy see, e.g., Ref. 36. In the resonant scattering situation not only the real parts, but also the imaginary parts of the potential curves V_+ and V_- are helpful in the understanding of the computed cross sections. At first sight it seems peculiar that we do not observe any sharp peaks in Figs. 5 and 6 although one of the discrete states couples very weakly to the continuum, i.e., Γ_{11} is very small. A glance at the corresponding Im $V_\pm$ in Figs. 1A and 1B explains this peculiarity which is typical for vibronic coupling situations. Except for a range of Q_u symmetric about $Q_u = 0$, where Re V_+ and Re V_- are close to each other, one finds that Im $V_+ \approx$ Im $V_- \approx (\Gamma_{11} + \Gamma_{22})/2$. In other words, if a narrow resonance interacts vibronically with a broad one, the resulting widths of the adiabatic resonances take on the mean value of the original widths and no sharp peaks will occur. It is only the region around $Q_u = 0$ or, more precisely, those vibrational wave functions which have considerable contributions in this region, to which this picture does not apply. On the other hand, the nonadiabatic operator (see Secs. III C and IV A) is most effective at the degeneracy points and will lead to a mixing of these vibrational wave functions of V_+ and V_- and thus tend to equalize the widths.

In the examples corresponding to Figs. 5 and 6, Γ_{11} has been chosen to be small compared to the vibrational frequency ω_u and the opposite is true for Γ_{22}. Their mean value is the same as in our first example where both widths have been set equal. By comparing the cross sections in Figs. 5 and 6 with those of the first example, Fig. 4, we indeed observe the peaks to be of comparable width in all three figures. In Fig. 6 this applies in particular to the peaks of the first hump which correspond to wave functions of the double-well curve Re V_-.

In the following we investigate the influence of an additional vibrational degree of freedom on the nuclear dynamics in vibronically coupled resonances. We employ the full Hamiltonian (38) and choose the widths to be functions of energy but independent of the nuclear coordinates. The nuclear dynamics is thus governed by a nonlocal potential. We choose

This article is copyrighted as indicated in the article. Reuse of AIP content is subject to the terms at: http://scitation.aip.org/termsconditions. Downloaded to IP: 130.89.98.137 On: Sun, 30 Nov 2014 02:07:35

$$\Gamma_{pp}(E) = a_p E^{(2l+1)/2} \exp\{-b_p E\} \quad (47)$$

which fulfills Wigner's threshold law[62] for scattering dominated by l waves at threshold in the absence of long-range forces. The real part $\Delta_{pp}(E)$ of the complex level-shift $F_{pp}(E)$ can be calculated via the Hilbert transform of $\Gamma_{pp}(E)$ according to Eq. (9c). For the specific width function in Eq. (47) the level-shift function is explicitly given in Ref. 49. The use of width functions which fulfill the threshold law is particularly important for resonances which overlap the threshold.[42] The vibronic coupling mechanism intermingles the diabatic resonances and may drastically change the behavior of the cross sections in the vicinity of the threshold as a function of energy and channel number. Here, we shall not further pursue this point.

Because of the large number of parameters entering the model Hamiltonian (38), a discussion of all the relevant multimode effects contained in it is not possible. Since we present here the first two-mode nuclear dynamics calculation in coupled resonances, we concentrate on a single example which brings to light an interesting vibronic phenomenon.

Figure 7 shows integral cross sections for the vibrational excitations $(0,0) \rightarrow (n_g, n_u)$ of the totally symmetric and nontotally symmetric modes. The parameters used in the computations are listed in the figure caption. Except of the widths, all the relevant parameters are taken from a realistic bound-state example which has been investigated previously.[36] In the absence of vibronic coupling, the inelastic cross sections for odd quantum numbers n_u of the nontotally symmetric mode vanish. In this case the elastic scattering cross section consists of two humps centered at E_1 and E_2 corresponding to the two diabatic resonance states. Since $\Gamma_{11}(E_1)$ is considerably smaller than $\Gamma_{22}(E_2)$, the hump at lower energy is much narrower than that at higher energy. The vibronic coupling mechanism is a very efficient mechanism for the excitation of nontotally symmetric modes. Figure 7 demonstrates that even for moderate interstate and intrastate coupling the excitation of a single quantum number of the nontotally symmetric mode can easily be stronger than that of the totally symmetric mode. The elastic cross section in the presence of vibronic coupling again exhibits two humps. As can be seen in Fig. 7 these humps overlap strongly. In particular, a third hump which is masked by substructures emerges between these two humps. This central hump originates from the partial cross section $\sigma_{22}(E)$ and the substructure from $\sigma_{11}(E)$. The appearance of a three hump structure is nicely documented by the $(0,0) \rightarrow (0,1)$ excitation function shown in Fig. 7. For other choices of parameters we have obtained a more pronounced central hump.

The existence of a central hump is a multimode vibronic effect. To underline this finding we have repeated the computation using the same set of parameters but discarding the totally symmetric mode, i.e., $\kappa_1 = \kappa_2 = 0$. The results obtained for this single-mode problem are shown in Fig. 8 for the elastic and first inelastic channels. There is no indication for a central hump in both cross section.

The different relative heights of the two humps in Fig. 8 and the two terminal humps in Fig. 7 is eyecatching for the elastic channel. Whereas both humps in the two-mode case and the first hump in the single-mode case ascend to about 5 Å^2, the second single-mode hump reaches 10 Å^2. This difference in relative heights becomes much more spectacular for other values of the model parameters. This phenomenon is a typical multimode vibronic coupling phenomenon.

In the single-mode situation the upper potential curve Re V_+ is steep, giving rise to large spacings of the vibrational levels. Since Re V_+ is more or less parallel to the ground state curve $V_0(Q_u)$, only a few of these levels are accessible in elastic scattering owing to the rapid decrease of the Franck–Condon factors with growing quantum numbers. Because of the vibronic coupling these vibrational levels interact with

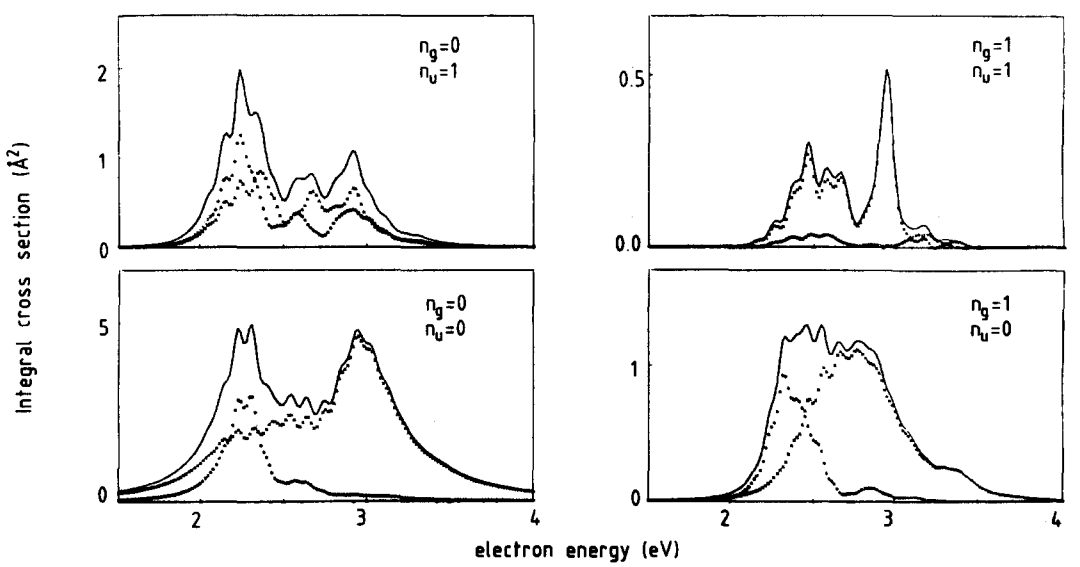

FIG. 7. Integral cross sections for the two-mode nonlocal problem (solid lines). n_g and n_u are the final quantum numbers of the totally and nontotally symmetric mode, respectively. Partial integral cross sections are also shown: $\sigma_{11}(E)$ and $\sigma_{21}(E)$ as circles and $\sigma_{22}(E)$ and $\sigma_{12}(E)$ as crosses. The values of the parameters are: $E_1 = 2.45, E_2 = 2.85, \lambda = 0.318, \kappa_1 = -0.212, \kappa_2 = 0.254, \omega_g = 0.258, \omega_u = 0.091, a_1 = 0.086, a_2 = 0.186$, all in eV, and $b_1 = 0.833\ \text{eV}^{-1}$, $b_2 = 0.375\ \text{eV}^{-1}$. Note that a_p and b_p are used to define the energy dependent width $\Gamma_{pp}(E)$ in Eq. (47).

This article is copyrighted as indicated in the article. Reuse of AIP content is subject to the terms at: http://scitation.aip.org/termsconditions. Downloaded to IP: 130.89.98.137 On: Sun, 30 Nov 2014 02:07:35

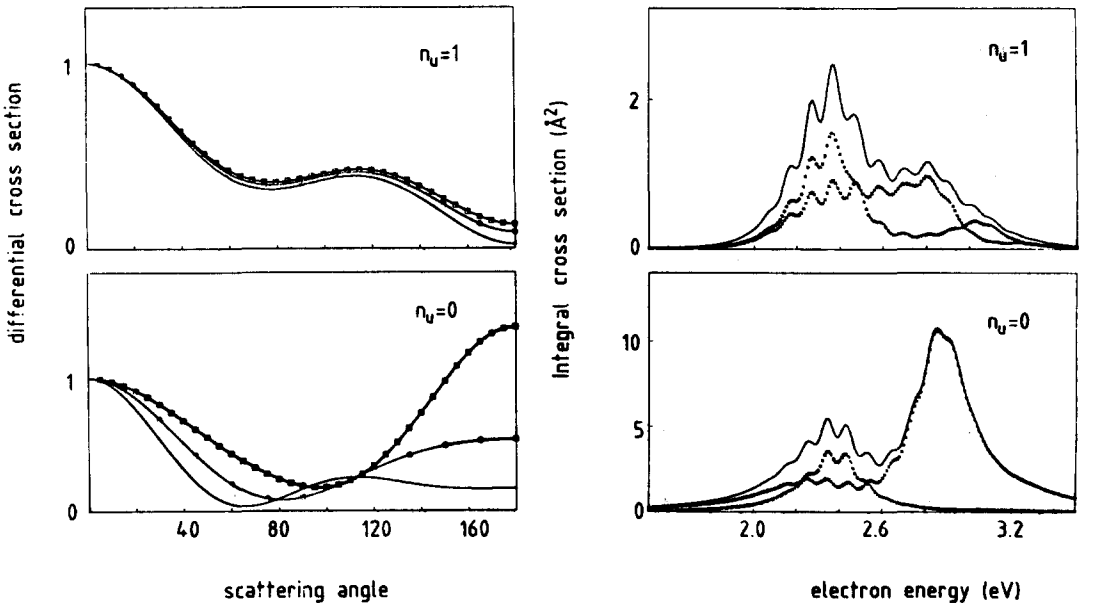

FIG. 8. Integral and differential cross sections for the single-mode nonlocal problem corresponding to Fig. 7. Only the coupling mode is considered and the effect of the totally symmetric mode is discarded. The differential cross sections normalized to unity at $\theta = 0°$ are shown for three values of the electron energy: $E = 2.3$ eV (solid curve), $E = 2.7$ eV (solid curve with squares), and $E = 3.1$ eV (solid curve with a few circles). For further details see caption of Fig. 7.

vibrational levels of Re V_- which are close by in energy and their "intensity" is spread over the resulting *vibronic* levels. The situation is similar in the multimode case except that the effects are much more pronounced. The density of vibrational levels of Re V_- at the levels of Re V_+ which are well accessible is much higher and the magnitude of the nonadiabatic effects is enhanced due to the presence of a square-root intersection of $V_+(Q_g,Q_u)$ and $V_-(Q_g,Q_u)$ as has been described in Sec. IV A (see also Figs. 2 and 3). Consequently, the intensity of the vibrational levels of Re V_+ is spread over numerous vibronic levels. According to Eq. (43) the overlap of the vibrational ground state $|0,0\rangle$ with these vibronic states enters the expression for the cross section in the *fourth* power which explains why the hump at high energy originating from V_+ is much higher in the single-mode case. Of course, the arguments brought above suffer somewhat from the fact that the imaginary parts of V_+ and V_- are also of importance. Nevertheless, they have been found to be applicable to explain the computed results at least qualitatively. In particular, the vibronic coupling mechanism tends to equalize the widths. If the widths are equal and constant, their influence on the cross sections is trivial and the above arguments fully apply. Finally, we mention that similar effects are present in the spectroscopy of related multimode

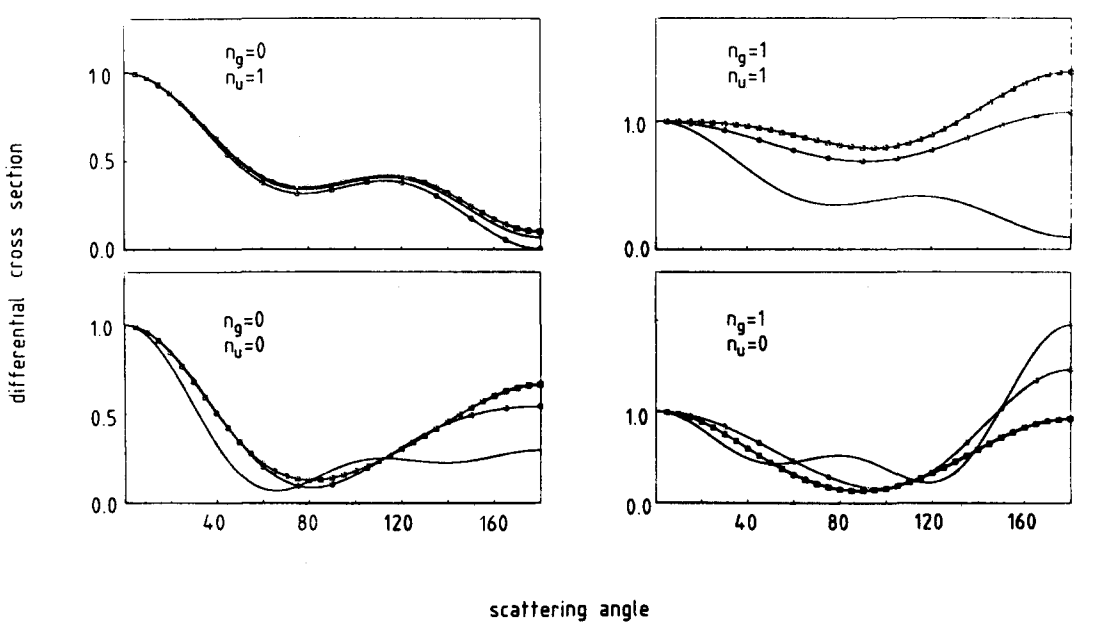

FIG. 9. Differential cross sections for the nonlocal two-mode problem of Fig. 7. The cross sections are normalized to unity at $\theta = 0°$. They are shown for three values of the electron energy: $E = 2.3$ eV (solid line), $E = 2.7$ eV (solid line with squares), and $E = 3.1$ eV (solid line with a few circles). For further details consult caption of Fig. 7.

This article is copyrighted as indicated in the article. Reuse of AIP content is subject to the terms at: http://scitation.aip.org/termsconditions. Downloaded to IP: 130.89.98.137 On: Sun, 30 Nov 2014 02:07:35

bound state systems.[36] In spectroscopy, however, the effects are less pronounced as the line intensity is related to the *second* power of the above mentioned overlap of states.

The normalized differential cross sections corresponding to the integral ones of Fig. 7 are shown in Fig. 9 for three different electron energies. For the elastic and the $n_u = 1$ first inelastic channel the differential cross sections are very similar to those found in our second and third single-mode examples. This is partly due to the fact that, as in these examples, the partial cross section $\sigma_{22}(E)$ is large everywhere and that $\sigma_{21}(E)$ and $\sigma_{12}(E)$ are of comparable magnitude. The normalized differential cross sections for the (0,0)→(1,0) and (0,0)→(1,1) excitations exhibit a more remarkable energy dispersion. The behavior of the partial cross sections reflects this energy dispersion. The quantity $\sigma_{22}(E)$ for the former excitation falls off more rapidly at lower energies than for the elastic scattering and $\sigma_{12}(E)$ is surprisingly small in the central part of the cross section for the latter excitation. It should be mentioned that, in general, the differential cross sections for the higher channels may depend more strongly on energy and on the scattering angle than those for the lower channels. For the (0,0)→(2,1) excitation of the present example, for instance, the normalized differential cross section grows by a factor of 10 at $E = 3.1$ eV but falls off to nearly zero at $E = 2.3$eV when going from $\theta = 0$ to $\theta = \pi$.

V. BRIEF SUMMARY

The nuclear dynamics in coupled resonance states is governed by an effective, complex, energy dependent, and nonlocal matrix potential. This potential describes two different coupling mechanisms. The resonances may interact via the coupling to the nonresonant scattering continuum and via the direct vibronic coupling of the discrete states out of which they emerge. In the present work the latter mechanism is discussed in greater detail.

The computation of the nuclear dynamics in the vibronically coupled resonance states for real systems involves an enormous numerical effort because of the complicated nature of the potential involved. To simplify the problem, local approximations are discussed. Furthermore, the local potential and in particular the complex adiabatic potential surfaces associated with it allow for the interpretation of the complicated nuclear dynamics within the combination of common frameworks used in the discussion of isolated resonance states and of the vibronic coupling in bound states.

To learn about the influence of the vibronic coupling mechanism on the vibrational excitation of molecules by resonant electron impact, a model is introduced which allows the computation of the nuclear dynamics for two modes in a nonlocal energy dependent potential. The model is an extension of a model which has been successfully applied to vibronic coupling of bound states. The results obtained for a few examples are discussed. Particularly interesting is the vibronic coupling between a narrow and a wide resonance. In this "competition" the wide resonance wins in the sense that there is a tendency for the narrow peaks to widen considerably due to the interaction. In general it is found that the vibronic coupling between resonances provides an efficient mechanism for the excitation of odd quanta of nontotally symmetric modes by resonant electron scattering. Vibronic coupling can markedly influence the angular distribution of the scattered electrons and the behavior of the vibrational excitation cross sections at threshold.

Of course it is desirable to analyze the nuclear dynamics in vibronically coupled resonances for a real molecule. To do so requires detailed fixed-nuclei data obtained, preferably by *ab initio* methods, on the discrete states and their coupling to the continuum and/or detailed experimental scattering data, e.g., vibrational excitation functions for various modes. These data are not yet available for a suitable molecule. The present investigation may help to identify the vibronic coupling effects and provides a first insight into the nature of the underlying interesting mechanism.

ACKNOWLEDGMENTS

The authors acknowledge helpful discussions with H. S.Köppel. This work has been supported by the Deutsche Forschungsgemeinschaft through SFB 91, the Fonds der Chemischen Industrie, and the Deutscher Akademischer Austausch-Dienst (Hérnan Estrada).

APPENDIX A: EXPLICIT EXPRESSIONS FOR THE ANGULAR FACTORS

In this appendix we quote the results obtained for the angular factors introduced in Eq. (17) under the condition that for each isolated resonance the scattering is in a single partial wave, l_p, in the molecule-fixed frame, i.e.,

$$V_{pk} = V_{pe} Y_{l_p}^{m_p}(\hat{k}), \tag{A1}$$

where p indicates the discrete state $|d_p\rangle$. Equation (A1) has to be transformed to the laboratory frame to compute the differential cross section. In linear molecules account must be taken of the orbital angular momentum $m_\pm$ about the axis, where for $m \neq 0$ the subscript + or − distinguishes between the two possible directions. The differential cross sections are obtained by averaging those in Eq. (12) over the molecular orientations $\hat{R}$,

$$\left(\frac{d\sigma}{d\Omega}\right)_{n_u\text{even}} = \frac{(2\pi)^4}{k^2}\frac{1}{4\pi}\int d\hat{R}\,|T_{11} + T_{22}|^2, \tag{A2}$$

$$\left(\frac{d\sigma}{d\Omega}\right)_{n_u\text{odd}} = \frac{(2\pi)^4}{k^2}\frac{1}{4\pi}\int d\hat{R}\,|T_{12} + T_{21}|^2. \tag{A3}$$

In the case $m \neq 0$ care must be taken to superimpose the T-matrix elements for all possible values of m.

Inserting Eq. (A1) into Eq. (11) and using the usual relations for the spherical harmonics we obtain the following expressions for the differential cross sections:

$$\left(\frac{d\sigma}{d\Omega}\right)_{n_u\text{even}} = \frac{\pi}{2E}\{\, g_{11}(\theta)|T_{11}(E)|^2 + g_{22}(\theta)|T_{22}(E)|^2 + 2g_{12}(\theta)\mathrm{Re}[T_{11}(E)T_{22}^*(E)]\}, \tag{A4}$$

$$\left(\frac{d\sigma}{d\Omega}\right)_{n_u\text{odd}} = \frac{\pi}{2E}\{f(\theta)[|T_{12}(E)|^2 + |T_{21}(E)|^2] + 2f_{12}(\theta)\mathrm{Re}[T_{12}(E)T_{21}^*(E)]\}. \tag{A5}$$

All angular factors are determined as linear combinations of Legendre functions $P_L(\cos\theta)$,

This article is copyrighted as indicated in the article. Reuse of AIP content is subject to the terms at: http://scitation.aip.org/termsconditions. Downloaded to IP: 130.89.98.137 On: Sun, 30 Nov 2014 02:07:35

$$g_{pq}(\theta)=\sum_L A_L^{pq}P_L(\cos\theta), \tag{A6}$$

$$f(\theta)=\sum_L B_L P_L(\cos\theta), \tag{A7}$$

$$f_{12}(\theta)=\sum_L C_L P_L(\cos\theta). \tag{A8}$$

The coefficients are given by the following equations:

$$A_L^{pq}=[X_{pq}^{pq}]^2\sum_{m_p m_q}\begin{pmatrix} l_p & l_q & L \\ m_p & -m_q & m_q-m_p\end{pmatrix}^2, \tag{A9}$$

$$B_L=X_{12}^{11}X_{12}^{22}\sum(-1)^{m_p+m_p'}\times\begin{pmatrix} l_1 & l_2 & L \\ m_p & -m_q & m_q-m_p\end{pmatrix}\begin{pmatrix} l_1 & l_2 & L \\ m_p' & -m_q' & m_q-m_p\end{pmatrix}, \tag{A10}$$

$$C_L=[X_{12}^{12}]^2\sum(-1)^{m_p-m_p'}\times\begin{pmatrix} l_1 & l_2 & L \\ -m_p & m_q & m_p-m_q\end{pmatrix}\begin{pmatrix} l_1 & l_2 & L \\ m_p' & -m_q' & m_p-m_q\end{pmatrix}, \tag{A11}$$

where

$$X_{p'q'}^{pq}=\alpha_{p'}\alpha_{q'}\left[\frac{(2L+1)(2l_{p'}+1)(2l_{q'}+1)}{2}\right]^{1/2}\times\begin{pmatrix} l_p & l_q & L \\ 0 & 0 & 0\end{pmatrix}. \tag{A12}$$

The constants α_1 and α_2 are determined by the conditions

$$\int g_{pp}(\theta)d\Omega=\int f(\theta)d\Omega=1. \tag{A13}$$

Note that

$$\int g_{12}(\theta)d\Omega=\int f_{12}(\theta)d\Omega=0. \tag{A14}$$

Equations (A6) to (A8) have been evaluated explicitly for several values of the quantum numbers l_1 and l_2. The results are collected in Table A1. In the numerical calculations discussed in Sec. IV B we have exclusively used $l_1=2$ ($m_1=\pm1$) and $l_2=1$ ($m_2=\pm1$). For linear symmetric molecules this choice corresponds to discrete states of Π_g and Π_u symmetry, respectively. These states may couple vibronically through a vibrational mode of Σ_u symmetry which does not lift the degeneracy of these states. In this case the computed cross sections $\sigma(E)$ should be multiplied by a factor of 2 to account for the degeneracy of the discrete states. Analogous factors must be introduced in other degeneracy situations. In particular, if the degeneracy is lifted by vibronic coupling, each component of the degenerate discrete states should appear as a state in the Hamiltonian $\mathscr{H}$.

APPENDIX B: MATRIX CONTINUED FRACTION METHOD

In this appendix we discuss the evaluation of the matrix elements of $\mathbf{C}\equiv(E\mathbf{1}-\mathscr{H})^{-1}$ in the basis $|n_g n_u\rangle$ which are the vibrational eigenstates of the target molecule. The effective Hamiltonian $\mathscr{H}$ is defined in Eq. (38). We may write

$$C_{11}=[E-H_1-U(E-H_2)^{-1}U]^{-1}, \tag{B1}$$

$$C_{21}=-(E-H_2)^{-1}UC_{11}=-C_{22}U(E-H_1)^{-1}, \tag{B2}$$

where the following abbreviations have been introduced ($p=1,2$):

$$H_p=E_p+\tilde{H}_0+\kappa_p Q_g+\Delta_{pp}(E-\tilde{H}_0)-i\Gamma_{pp}(E-\tilde{H}_0)/2, \tag{B3}$$

$$U=\lambda Q_u. \tag{B4}$$

The elements C_{22} and C_{12} are obtained from C_{11} and C_{21} by interchanging the subscripts 1 and 2 in Eqs. (B1) and (B2), respectively.

We begin with the evaluation of $\langle n_g n_u|C_{11}|00\rangle$. The derivation of the more general $\langle n_g n_u|C_{11}|m_g m_u\rangle$ can be done analogously. The evaluation is carried out in two steps. In the first step $\hat{R}_{n_u}\equiv\langle n_u|C_{11}|0\rangle$ is calculated and subsequently $\langle n_g|\hat{R}_{n_u}|0\rangle$. The hat on $\hat{R}_{n_u}$ and on other quantities to be introduced below is to remind that these quantities are operators in Q_g space. The starting point is the identity

$$\langle n_u|C_{11}^{-1}C_{11}|0\rangle=\langle n_u|0\rangle=\delta_{n_u0}. \tag{B5}$$

Inserting $\hat{1}=\Sigma|m_u\rangle\langle m_u|$ in between C_{11}^{-1} and C_{11} in the above identity, we readily notice that because of

$$\langle n_u|U|n_u'\rangle=\frac{\lambda}{\sqrt{2}}(\sqrt{n_u+1}\,\delta_{n_u,n_u'-1}+\sqrt{n_u}\,\delta_{n_u,n_u'+1}) \tag{B6}$$

only $m_u=n_u$ and $m_u=n_u\pm2$ contribute. This finding leads to the recursion relations

$$\hat{A}_{n_u}\hat{R}_{n_u}-\hat{B}_{n_u}\hat{R}_{n_u+2}-\hat{B}_{n_u-2}\hat{R}_{n_u-2}=\delta_{n_u0}, \tag{B7}$$

where

TABLE A1. Explicit expressions for the angular factors $g_{11}(\theta)$, $g_{22}(\theta)$, $g_{12}(\theta)$, $f(\theta)$, and $f_{12}(\theta)$. We define $x\equiv\cos\theta$. Note that interchanging the subscripts "1" and "2" leaves g_{12}, f and f_{12} unchanged and $g_{11}\leftrightarrow g_{22}$.

$l_1(m_1)$	$l_2(m_2)$	$4\pi g_{11}$	$4\pi g_{12}$	$4\pi f$	$4\pi f_{12}$
0(0)	1(0)	1	$\frac{1}{3}x$	1	x
1(0)	2(±1)	$\frac{1}{5}(1+2x^2)$	$\frac{1}{28}\sqrt{2}(5x+x^3)$	$\frac{1}{7}(2+x^2)$	$\frac{1}{7}(-x+4x^3)$
1(±1)	0(0)	$\frac{6}{25}(1+7x^2)$	$\frac{1}{4}x$	1	x
2(±1)	1(±1)	$\frac{1}{14}(1-3x^2+\frac{45}{4}x^4)$	$\frac{25}{33}\sqrt{2}(-x+\frac{63}{32}x^3)$	$\frac{1}{7}(2+x^2)$	$\frac{1}{7}(-x+4x^3)$

This article is copyrighted as indicated in the article. Reuse of AIP content is subject to the terms at: http://scitation.aip.org/termsconditions. Downloaded to IP: 130.89.98.137 On: Sun, 30 Nov 2014 02:07:35

$$\hat{A}_{n_u} = E - \hat{H}_1(n_u) - \frac{\lambda^2}{2}\left[\frac{n_u}{E - \hat{H}_2(n_u - 1)} + \frac{n_u + 1}{E - \hat{H}_2(n_u + 1)}\right], \tag{B8}$$

$$\hat{B}_{n_u} = \frac{\lambda^2[(n_u + 1)(n_u + 2)]^{1/2}}{2[E - \hat{H}_2(n_u + 1)]}, \tag{B9}$$

$$\hat{H}_p(m) = E_p + m\omega_u + \tilde{H}_{0g} + \kappa_p Q_g + F_{pp}(E - m\omega_u - \tilde{H}_{0g}). \tag{B10}$$

Apart from the zero-point energy, $\tilde{H}_{0g}$ is the usual harmonic oscillator Hamiltonian for the Q_g mode: $\tilde{H}_{0g}|n_g\rangle = n_g\omega_g|n_g\rangle$.

Once the element $\hat{R}_0$ is known, one obtains $\hat{R}_2$ from Eq. (B7) with the choice $n_u = 0$. The next element $\hat{R}_4$ is then obtained from the relation (B7) with $n_u = 2$, and so on. On the other hand, $\hat{R}_0$ can also be determined via the recursion relations (B7). By introducing a hypothetical maximum number for n_u in (B7) above which the $\hat{R}_{n_u}$ vanish, and making successive use of the recursion relations, we obtain

$$\hat{R}_0 = [\hat{A}_0 - \hat{B}_0[\hat{A}_2 - \hat{B}_2[\hat{A}_4 - \hat{B}_4[\cdots]^{-1}\hat{B}_4]^{-1}\hat{B}_2]^{-1}\hat{B}_0]^{-1} \tag{B11}$$

which is a continued fraction of operators in Q_g space.

The $\hat{R}_{n_u}$ for even numbers n_u are fully determined by Eqs. (B7) and (B11). For odd numbers n_u, on the other hand, all $\hat{R}_{n_u}$ vanish. This can be seen by inspection. The set of linear equations (B7) decouples into two subsets, one for odd and one for even numbers n_u. The former subset is homogeneous and its solutions are

$$\hat{R}_1 = \hat{R}_3 = \hat{R}_5 = \cdots = 0. \tag{B12}$$

Odd quantum numbers appear in the matrix elements of C_{21}. With the aid of Eqs. (B2) and (B6) one readily obtains

$$\langle n_u|C_{21}|0\rangle = -\frac{\lambda}{\sqrt{2}}[E - \hat{H}_2(n_u)]^{-1} \times [\sqrt{n_u}\,\hat{R}_{n_u-1} + \sqrt{n_u + 1}\,\hat{R}_{n_u+1}]. \tag{B13}$$

Because of Eq. (B12) the matrix elements of C_{21} vanish for even quantum numbers.

The numerical evaluation of $\langle n_g n_u|C_{pq}|00\rangle$ is now straightforward. In the first step of the calculation the operators $\hat{A}_{n_u}$ and $\hat{B}_{n_u}$ are represented as matrices in the basis of the harmonic oscillator states $|n_g\rangle$. In the second step the matrix continued fraction (B11) is computed to determine the matrix $\{\langle m_g|\hat{R}_0|m_g'\rangle\}$. Finally, the recursion relations (B7) are used in matrix representation to compute all other matrices $\{\langle m_g|\hat{R}_{n_u}|m_g'\rangle\}$. In the two-mode numerical calculations discussed in the present paper we have used 20 basis states $|n_g\rangle$ and computed, depending on the energy, up to 150 steps in the continued fraction. We have checked that the results are converged. In the single-mode cases the quantities $\hat{R}_{n_u}$ are, of course, c numbers and the calculations are very efficiently carried out with the aid of Eqs. (B7) and (B11).

[1] See, for example, C. L. Shoemaker and R. E. Wyatt, Adv. Quantum Chem. **14**, 169 (1981), and references therein.
[2] See, for example, J. L. Dehmer and D. Dill in *Electron-Molecule and Photon-Molecule Collisions*, edited by T. Rescigno, V. McKoy, and B. Schneider (Plenum, New York, 1979), p. 225.
[3] See, for example, R. E. Golden, Adv. At. Mol. Phys. **14**, 1 (1978); N. F. Lane, Rev. Mod. Phys. **52**, 29 (1980), and references therein.
[4] With electronically bound states we mean states which are stable with respect to electron emission in the fixed-nuclei approximation.
[5] K. D. Jordan and P. D. Burrow, Acc. Chem. Res. **11**, 341 (1978); ACS Symp. Ser. **162**, 1 (1981).
[6] P. D. Burrow (unpublished).
[7] M. Allan, Chem. Phys. **81**, 235 (1983).
[8] S. F. Wong and G. J. Schulz, Phys. Rev. Lett. **35**, 1429 (1975).
[9] M. Tronc, L. Malegat, R. Azria, and Y. Le Coat, J. Phys. B **15**, L253 (1982).
[10] S. Y. Chu and L. Goodman, J. Am. Chem. Soc. **97**, 7 (1975); J. Chandrasekhar, R. A. Kahn, and P. von R. Schleyer, Chem. Phys. Lett. **85**, 493 (1982); J. Pacansky, N. S. Dalal, and P. S. Bagus, Chem. Phys. **32**, 183 (1978).
[11] F. H. Mies, Phys. Rev. **175**, 164 (1968).
[12] A. U. Hazi, J. Phys. B **16**, L29 (1983).
[13] A. Z. Devdariani, V. N. Ostrovskii, and Yu. N. Sebyakin, Sov. Phys. JETP **49**, 266 (1979).
[14] F. H. Read, Proc. R. Soc. London **83**, 619 (1964).
[15] I. Ya. Ogurtsov and L. A. Kazantseva, J. Mol. Struct. **55**, 301 (1979).
[16] P. A. M. Dirac, Z. Phys. **44**, 585 (1927).
[17] V. Weisskopf, Ann. Phys. (Leipzig) **9**, 23 (1931).
[18] H. Feshbach, Ann. Phys. (New York) **5**, 357 (1958).
[19] U. Fano, Phys. Rev. **124**, 1866 (1961).
[20] M. S. Child, in *Atom–Molecule Collision Theory*, edited by R. B. Bernstein (Plenum, New York, 1979).
[21] H. C. Longuet-Higgins, Adv. Spectrosc. **2**, 429 (1961).
[22] H. Feshbach, Ann. Phys. (New York) **19**, 287 (1962).
[23] J. C. Y. Chen, Phys. Rev. **148**, 66 (1966); **156**, 12 (1967).
[24] T. F. O'Malley, Phys. Rev. **150**, 140 (1966).
[25] J. N. Bardsley, Proc. R. Soc. London **91**, 300 (1967); J. Phys. B **1**, 349 (1968).
[26] H. Nakamura, J. Phys. Soc. Jpn. **26**, 1473 (1969).
[27] F. Fiquet-Fayard, J. Phys. B **8**, 2880 (1975).
[28] W. Domcke and L. S. Cederbaum, Phys. Rev. A **16**, 1465 (1977).
[29] R. J. Bieniek, Phys. Rev. A **18**, 392 (1978).
[30] A. U. Hazi, T. N. Rescigno, and M. Kurilla, Phys. Rev. A **23**, 1089 (1981).
[31] W. Domcke and L. S. Cederbaum, in *Electron–Atom and Electron–Molecule Collisions*, edited by J. Hinze (Plenum, New York, 1983), p. 255.
[32] G. J. Schulz, Rev. Mod. Phys. **45**, 423 (1973).
[33] F. H. Read and G. L. Whiterod, Proc. R. Soc. London **85**, 71 (1965).
[34] I. Ya. Ogurtsov, L. A. Kazantseva, and A. A. Ischenko, J. Mol. Struct. **41**, 243 (1977).
[35] W. Domcke, M. Berman, H. Estrada, C. Mündel, and L. S. Cederbaum, J. Phys. Chem. **88**, 4862 (1984).
[36] H. Köppel, W. Domcke, and L. S. Cederbaum, Adv. Chem. Phys. **57**, 59 (1984).
[37] G. Herzberg and E. Teller, Z. Phys. Chem. (Leipzig) B **21**, 410 (1933).
[38] J. N. Bardsley and F. H. Read, Chem. Phys. Lett. **2**, 333 (1968).
[39] T. F. O'Malley and H. S. Taylor, Phys. Rev. **176**, 207 (1968).
[40] L. Dubé and A. Herzenberg, Phys. Rev. A **20**, 194 (1979).
[41] J. R. Taylor, *Scattering Theory* (Wiley, New York, 1972).
[42] L. S. Cederbaum and W. Domcke, J. Phys. B **14**, 4665 (1981).
[43] A. Herzenberg, J. Phys. B **1**, 548 (1968).
[44] G. Breit and E. P. Wigner, Phys. Rev. **49**, 519 (1936).
[45] M. Berman, L. S. Cederbaum, and W. Domcke, J. Phys. B **16**, 875 (1983).
[46] G. Herzberg, *Molecular Spectra and Molecular Structure*, (Van Nostrand, New York, 1966), Vol. III.
[47] H. Hong, J. Chem. Phys. **67**, 801 (1977).
[48] M. Cini, Phys. Rev. B **17**, 2486 (1978).
[49] M. Berman, H. Estrada, L. S. Cederbaum, and W. Domcke, Phys. Rev. A **28**, 1363 (1983).
[50] C. Mündel, M. Berman, and W. Domcke, Phys. Rev. A **32**, 181 (1985).
[51] A. U. Hazi, A. E. Orel, and T. N. Rescigno, Phys. Rev. Lett. **46**, 918 (1981).
[52] R. Englman, *The Jahn–Teller Effect* (Wiley, New York, 1972).
[53] I. B. Bersuker, *The Jahn–Teller Effect and Vibronic Interactions in Modern Chemistry* (Plenum, New York, 1984).

This article is copyrighted as indicated in the article. Reuse of AIP content is subject to the terms at: http://scitation.aip.org/termsconditions. Downloaded to IP: 130.89.98.137 On: Sun, 30 Nov 2014 02:07:35

[54]G. Herzberg and H. C. Longuet-Higgins, Discuss. Faraday Soc. **35**, 77 (1963).
[55]E. Teller, J. Phys. Chem. **41**, 109 (1937).
[56]T. Carrington, Acc. Chem. Res. **7**, 20 (1974).
[57]R. L. Fulton and M. Gouterman, J. Chem. Phys. **35**, 1059 (1961); **41**, 2280 (1964).
[58]W. Domcke and L. S. Cederbaum, J. Phys. B **13**, 2829 (1980).
[59]W. Domcke and L. S. Cederbaum, Chem. Phys. **25**, 189 (1977).
[60]W. Domcke and L. S. Cederbaum, J. Phys. B **10**, L47 (1977).
[61]F. T. Smith, Phys. Rev. **179**, 111 (1969).
[62]E. P. Wigner, Phys. Rev. **73**, 1002 (1948).
[63]Note the difference between the diabatic *discrete* states and diabatic *resonance* states. The former states are diabatic (Refs. 20 and 21) with respect to both the discrete–continuum coupling and the vibronic coupling, the latter are adiabatic with respect to the discrete–continuum coupling, but diabatic with respect to the vibronic coupling.

This article is copyrighted as indicated in the article. Reuse of AIP content is subject to the terms at: http://scitation.aip.org/termsconditions. Downloaded to IP: 130.89.98.137 On: Sun, 30 Nov 2014 02:07:35